INFLUENCE OF Ar-CO_2 MIXTURES

AND THIN ELECTRODES

ON METAL TRANSFER IN GAS METAL ARC WELDING

by

Erik J. Soderstrom

A thesis submitted to the Faculty and Board of Trustees of the Colorado School of Mines in partial fulfillment of the requirements for the degree of Master of Science in Metallurgical and Materials Engineering.

Golden, Colorado
Date 12-13-2006

Signed: Erik Soderstrom
Erik J. Soderstrom

Approved: PF Mendez
Dr. Patricio Mendez
Thesis Advisor

Golden, Colorado
Date 1/24/07

Dr. John Moore
Professor and Head
Department of Metallurgical
And Materials Engineering

ABSTRACT

The goal of this research is to reduce Gas Metal Arc (GMA) welding costs by using higher amounts of low-cost CO_2 in the shielding gas while keeping high weld quality and deposition rates. Previous attempts at this resulted in poor weld quality and high amounts of spatter due to repelled transfer of the metal droplets.

By using electrodes with diameters down to 0.016 in. at high wire feed speeds (1400 ipm), the metal transfer modes in a variety of binary Ar-CO_2 shielding gas mixtures were investigated. A special contact tip was designed for use with the 0.016 in. diameter electrode because no commercially produced tips were available. A United States patent for this design is pending, application # 2006/0237411.

It was found that droplet sizes do not decrease proportionally with wire sizes. Repelled transfer is dominant with shielding gas compositions containing more than 30% CO_2 regardless of wire diameter.

New observations have been made in metal transfer modes. By using small diameter electrodes (<0.035 in.) with shielding gases containing more than 70% argon, the mode has characteristics of both globular and spray. Droplet diameters never become smaller than electrode diameters, regardless of the current used. A lower limit exists on the size of droplets that is independent of the electrode size.

TABLE OF CONTENTS

LIST OF FIGURES

LIST OF TABLES

ACKNOWLEDGEMENTS

This work was supported by the American Welding Society through a research fellowship grant. Without their support, I would not have had the freedom to pursue any of the work presented in this thesis. I would like to express my appreciation to Bruce Albrecht of Miller Electric for his generous donations of equipment.

I would like to acknowledge the support and guidance of my advisor, Dr. Patricio Mendez. It has been a great pleasure working with him and his insight into the welding process has been invaluable.

I would like to thank the faculty of the Department of Metallurgical and Materials Engineering at the Colorado School of Mines for providing an excellent atmosphere for research and learning. My academic experience here has been both challenging and rewarding.

Finally, I want to express my deepest appreciation to my wife, Rebecca. Without her devotion, support, and encouragement, I would not be in the position I am today.

1. INTRODUCTION

Arc welding is a widely used manufacturing process used for joining metals. When compared to other joining processes, such as riveting or bolting, welded structures tend to be stronger, lighter-weight and cheaper to produce. Many types of arc welding exist, and Gas Metal Arc (GMA) welding is the most commonly used process today. The initial development of GMA welding focused on joining reactive metals such as aluminum and magnesium. These applications used pure argon to shield the molten metal from chemical reactions with atmosphere. High production rates and other benefits of this process became apparent quickly, and soon it was used in other applications such as the joining of mild steels. This process was continually improved. Beginning in the 1950s, researchers explored the effects that shielding gas composition had on the GMA welding process [1-3]. They found that welds of good quality could be made with additions of CO_2 to argon, and even with 100% CO_2 as the shielding gas. Carbon dioxide is less expensive and more available than argon, however, CO_2 welding has limitations, and the highest quality welds and largest deposition rates in GMA welding are still made with large percentages (>75%) of argon in the shielding gas.

This investigation explores a new approach that attempts to overcome these limitations and enables the use of inexpensive CO_2 shielding gas for high quality welds and large deposition rates. The sections that follow in this chapter include the motivation of the work, the method of investigation and limitations in scope. Following is a brief description of the organization of the thesis, which acts as a roadmap to the following chapters.

1.1. Purpose and Motivation

The primary purpose of this investigation is to reduce manufacturing costs by reducing the expenditures on welding consumables. The GMA welding process uses several consumables including electrodes, contact tips, and shielding gas. These are the most often replaced elements and make up a large portion of operating cost. In a report conducted at the Colorado School of Mines [4] , it was found that by switching from argon to CO_2, savings of up to $5,000 per year per welding machine may be realized. This is for an industrial welding machine that is operated for 8 hours a day, 300 days a year with a duty cycle of 35% assuming weld quality and deposition rates remain the same. But this is not the case because shielding gases containing binary mixtures of argon and CO_2 greatly influence the GMA welding process depending on their compositions. Mixtures containing less than 25% CO_2 are widely used because they produce high quality welds at high deposition rates. Mixtures with more than 25% CO_2 are used, but weld quality deteriorates at constant deposition rates. These mixtures are often used in GMA welding for applications that do not require the highest deposition rates and weld quality.

The new method proposed in this work will address this dilemma and try to use high concentrations of CO_2 and high deposition rates to maximize the possible cost savings.

1.2. Method of Investigation

This work examines experimentally the behavior of GMA welding with varying amounts of CO_2 and argon in the shielding gas. What differentiates this work from all previous is that the behavior of very thin electrodes (down to 0.016 in. diameter) is explored. The experimental techniques include a combination of high-speed laser shadowgraph techniques and signal analysis of welding current and voltage. These methods have been used during previous investigations [5-9] and have been proven to be very reliable.

1.3. Limitations in Scope

The welds performed during this study are made using Direct Current Electrode Positive (DCEP). No programmable waveforms for pulsed current are investigated. Commercially bought electrodes are utilized. No chemical coatings or other pre-weld treatments are given to the wire. Characterization of metal transfer mode and process stability is the goals of the investigation. Post-weld process characterization such as mechanical testing and microstructural analysis are not performed.

1.4. Organization of Thesis

Chapter 2 describes several unique features of the GMA welding process. It begins with an overview of the system. Next, metal transfer modes are defined and discussed. The physics involved with droplet detachment are presented, along with the welding variables that affect the operation of the GMA welding process.

Chapter 3 presents more detailed information on metal transfer characteristics and the effects of CO_2 in the shielding gas. This chapter contains previous experimental and theoretical analyses that pertain to the scope of this research.

Chapter 4 builds on the previous observations to develop the hypothesis. It is suggested that by using small diameter electrodes, more CO_2 can be used in the shielding gas and still produce high-argon quality welds at high deposition rates.

Chapter 5 presents the experimental procedure. The chapter begins with a discussion of the experimental apparatus that was fabricated to run tests. The experimental testing method that was used to collect data follows.

Chapter 6 contains the results and discussion. The data collected is presented in graphical form. Droplet detachment frequencies and droplet diameters are given for different currents, wire diameters, and shielding gas compositions. Trends are analyzed and discussed and the results are summarized. Limitations of the methods as well as implications of the results are presented.

Chapter 7 presents the conclusions that were found through this research and the recommendations for future work.

2. GMA WELDING OVERVIEW

The objective of this chapter is to introduce the various aspects of metal transfer phenomena that occur during GMA welding. First, the fundamentals of GMA welding are presented. Then, classification of metal transfer is given, followed by an analysis of the forces that influence the metal transfer behavior. Finally, the welding parameters that influence metal transfer are presented.

2.1. GMA Welding Fundamentals

A schematic diagram of a basic gas metal arc welding setup is shown in Figure 2.1. GMA welding uses a continuous metal electrode wire that is fed into an electric arc. The arc is maintained between the electrode and the baseplate and is controlled by the welding power source. The heat produced from the arc melts both the baseplate and the electrode, coalescing in the molten weld pool. As the heat from the arc moves along the travel direction, the trailing weld metal solidifies and the completed weld is left.

Molten drops produced at the end of the electrode are transferred across the arc into the weld pool. The droplets can be transferred across the arc in a variety of ways, depending on factors such as current, voltage, shielding gas composition, electrode diameter, chemical composition of the electrode, and several others.

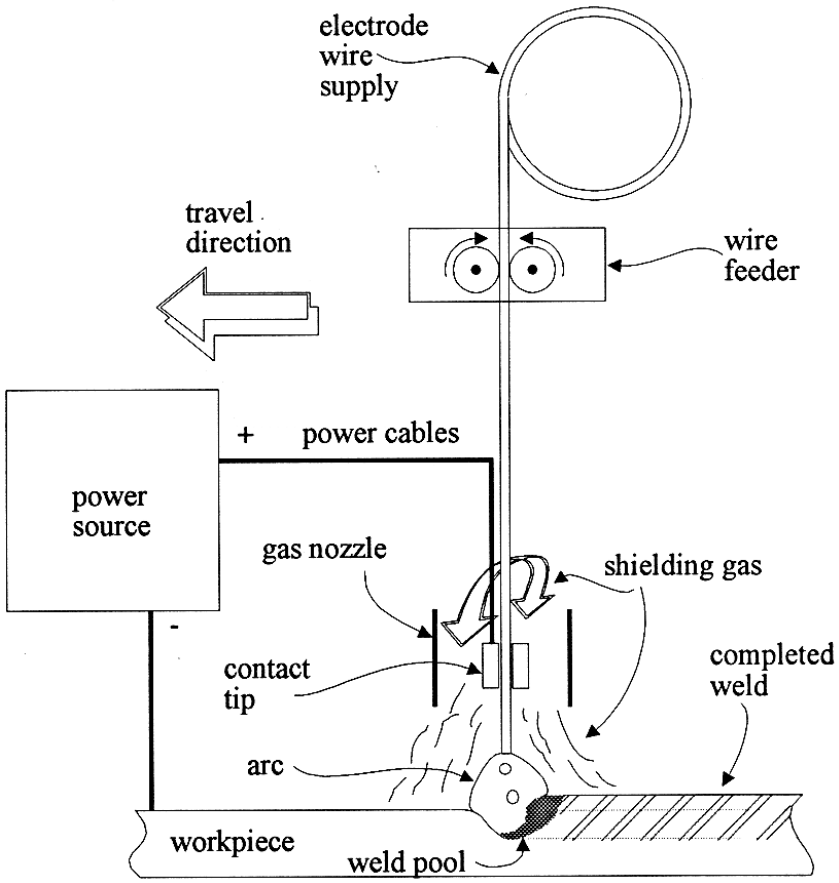

Figure 2.1. Schematic of a typical GMA welding system.[10]

Figure 2.2 shows the primary input variables and terminology for a standard GMA welding setup in the near-arc region. Wire feed speed (WFS) and process voltage are the adjustable inputs on the power source. By adjusting these, the welding current and arc length can be varied. From Figure 2.2, electrode extension or stick-out is the length of electrode measured from the distal end of the contact tip to the arc. The summation of arc length and electrode extension gives the contact tip to work distance (CTWD). Shielding gas composition and CTWD can be directly controlled with a gas mixer and adjustable fixture, respectively.

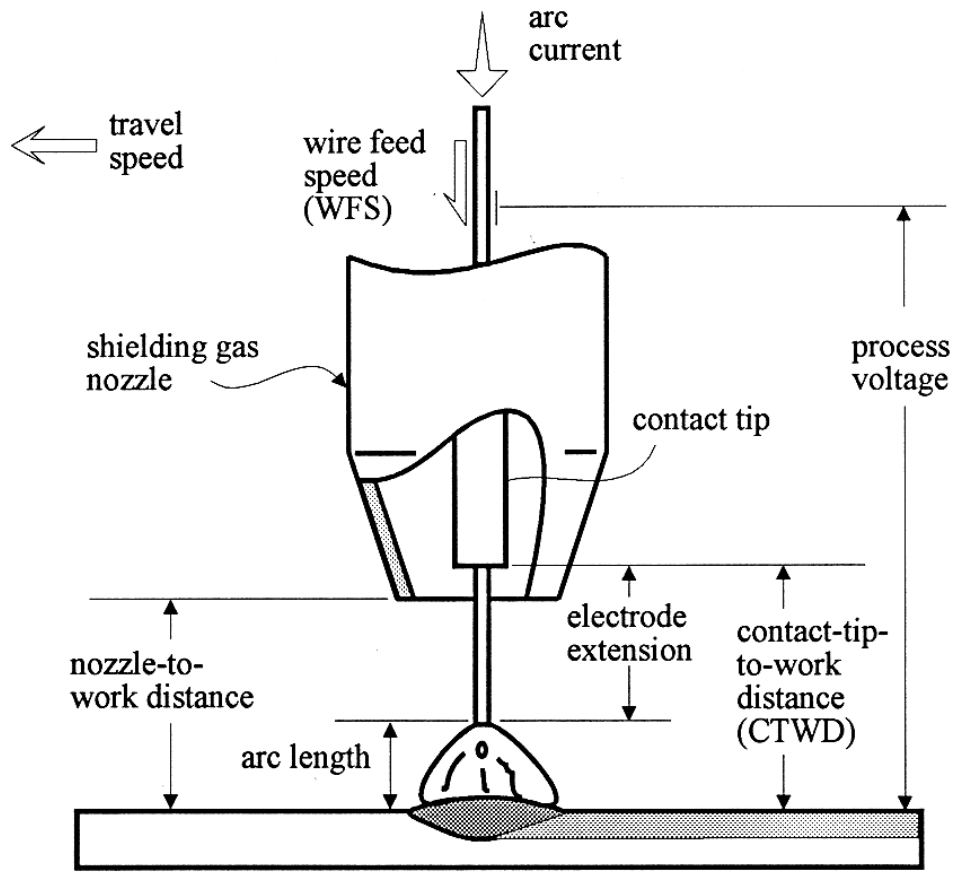

Figure 2.2. GMA welding parameters and terminology. [10]

2.2. Classification of Metal Transfer

During operation, the consumable electrode wire is continuously fed into the arc. In this region, sufficient energy exists to melt both the wire and the base metal. The molten metal at the tip of the electrode can be transferred across the arc in a variety of ways. Lancaster [11] wrote one of the most comprehensive reviews on the transfer of metal during GMA welding. Brandi [12] gives a good overview on the different techniques for observing metals transfer. In this research, both high speed video and

current and voltage analysis are used. The International Institute of Welding (IIW) has classified this metal transfer into different categories. They are shown schematically in Figure 2.3, and can be divided into three distinct groups: free flight transfer, short-circuiting transfer, and slag-protected transfer.

The electrode never contacts the weld pool during free flight transfer; molten droplets detach from the electrode, travel through the arc, and are deposited in the weld pool. The manner in which the droplets are transferred depends on several variables. Wire diameter, chemical composition, shielding gas composition, current and voltage all influence the metal transfer mode. At low currents in an argon-rich atmosphere, drop or globular transfer is dominant. As current increases, the metal transfer mode shifts from drop to projected spray transfer. Further increases in current lead to streaming spray transfer. At even higher current levels, the metal transfer changes to rotating spray transfer. The repelled transfer illustration shown in Figure 2.3 occurs when large amounts of CO_2 (greater than 25%) or helium are in the shielding gas.

During short-circuiting transfer, the electrode periodically contacts the weld pool. During this contact, the arc is briefly extinguished. Short-circuiting transfer is used with lower currents than free-flight transfer. Explosive transfer may happen with higher welding currents, causing the electrode to explode due to the amount of power being supplied. This is similar to a fuse rupturing due to excess amounts of current. Slag-protected transfer occurs in welding processes that involve large quantities of fluxes, such as submerged arc welding, and is not applicable to this study. Further classification is given in Table 2.1.

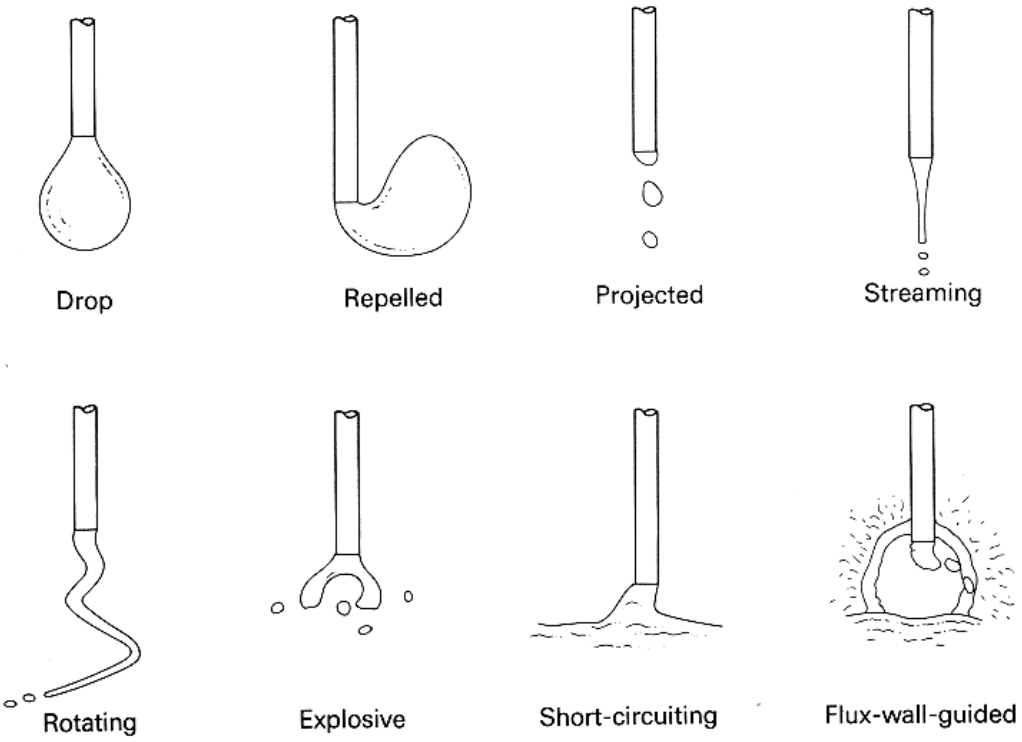

Figure 2.3. Metal transfer modes in arc welding according to IIW classifications. [11]

Table 2.1. International Institute of Welding Classifications of Metal Transfer. [13]

Designation of Transfer Type		Welding Process (examples)
1.	Free-flight transfer	
1.1	Globular	
1.1.1	Drop	Low-current GMA
1.1.2	Repelled	CO_2 shielded GMA
1.2	Spray	
1.2.1	Projected	Intermediate-current GMA
1.2.2	Streaming	Medium-current GMA
1.2.3	Rotating	High-current GMA
1.3	Explosive	SMA (covered electrodes)
2.	Bridging transfer	
2.1	Short-circuiting	Short-circuiting GMA
2.2	Bridging without interruption	Welding with filler metal addition
3.	Slag-protected transfer	
3.1	Flux-wall guided	SAW
3.2	Other modes	SMA, cored wire, electroslag

2.3. Metal Transfer Physics

In order to explain the different types of metal transfer, researchers have investigated the forces acting on the droplet. [14-18] It is widely accepted that four forces act upon the droplet during GMA welding: gravity F_g, an aerodynamic drag force due to the flow of shielding gas around the drop F_d, surface tension force F_γ, and the electromagnetic force F_{em}. These can be classified as attaching or detaching forces depending on the welding variables. The next sections will investigate each of these forces individually to show how they are derived. Most of these forces are dependent on geometries in the detachment region. Figure 2.4 shows several of the variables used in the determination of these forces. In the figure, R is the radius of the molten droplet and α is smallest radius in the necking region.

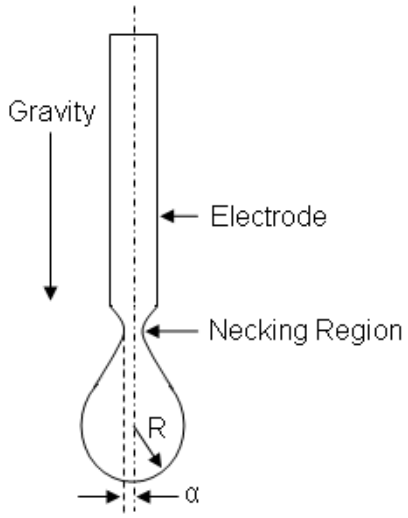

Figure 2.4. A schematic representation of the variables used in the calculations of forces during droplet detachment.

2.3.1. Gravity

For welds made in the flat position, gravitational force assists with droplet detachment; it is a detaching force. Although the pendent drop does not have an exact spherical shape, its weight can be approximated as if it were. Assuming a spherical droplet hanging from the tip of the electrode, the weight of the droplet is:

$$F_G = \frac{4}{3}\pi R^3 \rho_d g \qquad 2.1$$

where R is the radius of the droplet, ρ_d is the density of the droplet, and g is the acceleration of gravity.

2.3.2. Surface Tension

The surface tension force retains the droplet on the electrode (attaching force). Similar surface tension effects are seen with a dripping faucet. The force is given by Kim [18] as:

$$F_\gamma = 2\pi\alpha\gamma \qquad 2.2$$

where α is the radius of the necking region shown in Figure 2.4 and γ is the surface tension of the liquid metal at the neck. Chemical composition of the electrode and any active gases in the arc atmosphere will affect the surface tension value. In this study, CO_2 is an active gas, which means that it will dissociate in the plasma. The resulting free oxygen and carbon will decrease the surface tension of the liquid metal.

2.3.3. Aerodynamic Drag Force

To prevent chemical reactions between molten metal and atmosphere, a shielding gas is directed through the torch tip. The gas displaces the air in the vicinity around the droplet and weld pool. Flows ranging from 20-50 cfh are typically used. These gas flows act upon the droplet, creating an aerodynamic drag force that assists in detaching the droplet from the electrode. It is given as:

$$F_d = \frac{\pi}{2} v^2 \rho_g R_d^2 C_d \qquad 2.3$$

where v is the fluid stream velocity, ρ_g is the density of the flowing medium, R_d is the radius of the sphere immersed in the fluid stream, and C_d is the drag coefficient. Because of the attachment to the wire, C_d is more complex than that for a detached sphere in free flow.

2.3.4. Electromagnetic Pinch Force

GMA welding uses electricity to supply the energy needed to melt and subsequently fuse metals together. The power supply used in this study creates a constant voltage direct current (CV/DC) waveform that operates between 10-50 volts and 50-500 Amperes, depending on welding variables. In this electrical circuit, the main area of interest is the region between the contact tip and the baseplate, which contains the electrode and the arc. Both of these elements carry current and have an associated electromagnetic (EM) field. This EM field gives rise to electromagnetic force which has a significant effect on metal transfer, and is referred to as the Lorentz force. The generalized equation for the Lorentz force is:

$$F_{em}=\boldsymbol{J} \times \boldsymbol{B} \qquad 2.4$$

where $\boldsymbol{J}$ is the current density vector and $\boldsymbol{B}$ is the electromagnetic field density vector. Current density is an important factor that influences metal transfer. The self-induced EM field vector, shown in Figure 2.5 is concentric about the wire. The Lorentz force is the cross product of these two vectors and results in a radial inward pinch force. This pinch force is not only present in the electrode, but also in the plasma. Further analysis of Equation 2.4 has shown the force to be:

$$F_{em} = \frac{I^2}{200}\ln(\frac{A_a}{A_e}) \qquad 2.5$$

where I is the welding current, A_e is the area of the solid electrode, A_a is the area of the anode spot. The factor of 200 gives the resulting electromagnetic force in dynes (10^{-5} N). Depending on the ratio of these areas, the Lorentz force can be either attaching or detaching.

This simplified explanation has been expanded by researchers [19, 20] to account for experimental observations that include tapering of the molten electrode in an argon atmosphere and repelled transfer in CO_2 atmospheres.

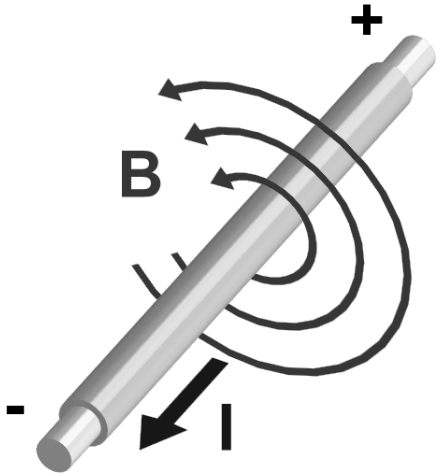

Figure 2.5. The self-induced electromagnetic field vector *B* is concentric and perpendicular to the current carrying wire.

The modeling associated with the pinch force is complex. As mentioned, Lorentz force is present in the droplet and in the plasma. The current densities associated with each of these regions, as well as the interface between them are not known. In turn, calculating the force balance is extremely difficult to do. To date, a general theory that is able to explain the phenomena associated with the Lorentz force has not been agreed upon. However, experimental observations and qualitative analysis enable better understanding of the forces at work.

2.4. Welding Parameters in GMA welding

The GMA welding process is able to produce high quality welds for a variety of different applications. This is due to the flexibility of welding parameters. This section covers the parameters associated with GMA welding and how they influence metal transfer and the forces described previously.

2.4.1. Current

During GMA welding, current is roughly proportional to the wire feed speed (WFS). It is one of the main inputs for current density and has a large influence on the magnitude of EM forces and the metal transfer mode. Current also contributes significantly to the resistive heating of the electrode extension.

2.4.2. Voltage

Voltage and arc length are often used interchangeably, but they are different. For a given welding setup, voltage and arc length vary in similar ways. However, for a given voltage, the arc length will change with shielding gas composition, current, and electrode extension. If all other variables remain constant, an increase the voltage setting will increase arc length. Voltage is a key element during process monitoring. Metal transfer can be characterized based on voltage variations, as shown by Lan [21]. Similar techniques are used in this research. Low voltage can result in short circuit transfer;

however, for free flight transfer, voltage does not play a significant role in the forces acting on droplets.

2.4.3. Electrode Extension

Electrode extension, commonly called stick-out, has a significant influence on the metal transfer modes due to the resistive heating in this region. Figure 2.6, taken from Lesnewich, illustrates an increase in extension results in greater resistive heating that contributes to greater electrode melting rates for a given current. Heald [22] showed similar results in his research.

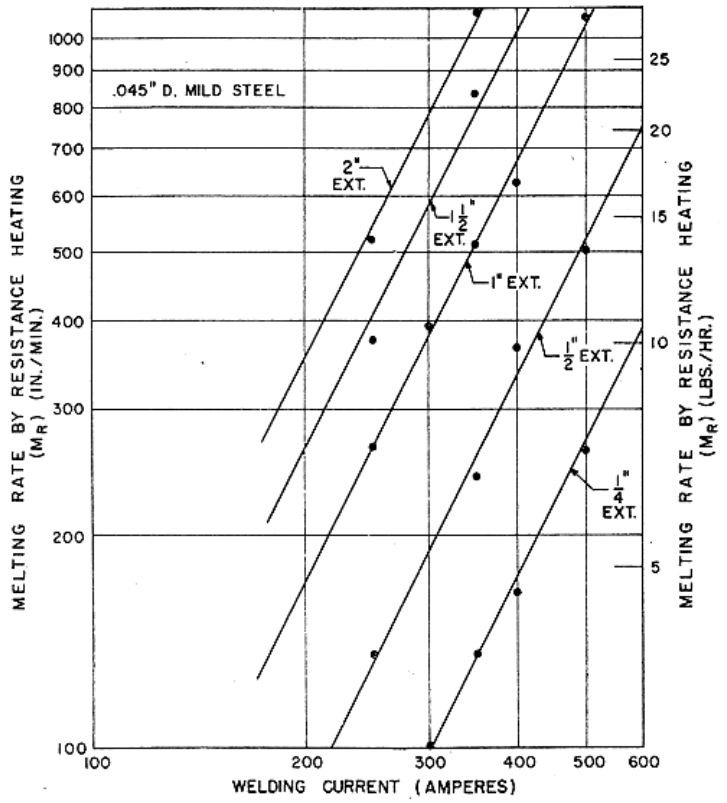

Figure 2.6. Effect of welding current and electrode extension on resistive heating. [23]

2.4.4. Shielding Gas

The shielding gas used has a significant effect on metal transfer. A variety of gases are available for use in the GMA welding process. Table 2.2 shows common shielding gases used along with their properties. Depending on the gas, it is classified as inert or active. Argon and helium do not react with the liquid metal, they are inert. Carbon dioxide, oxygen, hydrogen, and nitrogen are multiatomic molecules that dissociate when exposed to temperatures in the arc and are able to react with the metal. Many times, a mixture of gases is used that is suited for the particular application. The gas affects the plasma properties and the flow of current as it travels through the electrode and plasma which leads to changes in the Lorentz pinch force in both the plasma and the electrode. Gas composition also affects the surface tension of the metal. These effects will be discussed in greater detail in Chapter 3.

Table 2.2. Common shielding gases and their properties. [24]

Gas	Chemical symbol	Molecular weight	Specific gravity(a)	Density		Ionization potential	
				g/ft^3	g/L	aJ(b)	eV
Argon	Ar	39.95	1.38	0.1114	1.784	2.52	15.7
Carbon dioxide	CO_2	44.01	1.53	0.1235	1.978	2.26	14.4
Helium	He	4.00	0.1368	0.0111	0.178	3.92	24.5
Hydrogen	H_2	2.016	0.0695	0.0056	0.090	2.16	13.5
Nitrogen	N_2	28.01	0.967	0.782	12.5	2.32	14.5
Oxygen	O_2	32.00	1.105	0.0892	1.43	2.11	13.2

(a) At 100 kPa (1 atm) and 0 °C (32 °F); air = 1. (b) 10^{-18} J. Source: Ref 1

2.4.5. Chemical Composition

The alloying elements that are present in the electrode have a several effects on the forces acting on the droplet. First, different compositions of metal have different resistivities, which effects the amount of resistive heating that occurs in the stick-out. Second, chemicals such as sulfur and oxygen are surface active elements, which change the surface tension of the droplet and lead to changes in the surface tension force. The

chemical composition of the electrode will also affect the partial pressures of various elements. The partial pressures determine the amount of elements in the plasma, which have a large effect on fume generation as well as plasma-electrode interaction. The viscosity of the molten metal depends on the chemical composition. Lower viscosities will detach easier.

2.5. Summary

During the GMA welding process, a consumable electrode is fed into a high temperature electric arc. The molten droplets that subsequently evolve can have several morphologies, originating different metal transfer modes, which are dependent on the forces acting on the droplets. By controlling welding parameters, these forces can be manipulated and the desired metal transfer mode can be achieved. These concepts provide a basis that will enable understanding of the methodology presented in subsequent sections.

3. METAL TRANSFER RESEARCH AND CO_2 WELDING CHARACTERISTICS

The purpose of this chapter is to present a background on the research that has been done on metal transfer and the effects that CO_2 has on the welding process when used as an addition to the shielding gas. This chapter is divided into three main sections. The first section is the experimental and theoretical observations that have been made by other researchers on the transition phenomenon between globular and spray transfer, one of the focuses of this research. The second section of this chapter describes the influence of CO_2 during GMA welding. The third section describes methods that have been used to improve weld quality and deposition rates in CO_2 welding.

Since the commercial development of the GMA welding process in the late 1940s, researchers have continuously studied and characterized the observable facts associated with it [24]. Monitoring current, voltage, and droplet rates are the usual parameters. As described in Chapter 2, GMA welding involves numerous coupled variables, meaning that changing one often affects many others. Characterizing the relationships between variables is complex. For instance, current has a large influence on metal transfer mode, but so do electrode extension, voltage, electrode diameter, shielding gas composition, arc geometry, and many more. By understanding the relationships between these variables, the knowledge of the entire welding system is enhanced.

3.1. Characteristic Observations Regarding the Transition Region

As metal transfer modes change, other welding parameters change as well. Experienced welding operators rely on sight, sound, and feel to characterize and adjust

the welding process accordingly. Researchers do much of the same, but use sophisticated sensing equipment to quantify and analyze the effects of outputs such as current, voltage, audio and video. The following section presents previous research regarding changes that occur during the transition from globular to spray transfer mode.

3.1.1. Droplet Detachment Frequency

Lesnewich [25] noted during experimentation that a gradual increase in current produces an increase in the rate of drop detachment and a reduction in the drop size. However, this gradual change did not continue indefinitely. When the welding current is increased beyond a critical level, droplet size suddenly decreases, a sharp tip is formed at the end of the electrode and droplet detachment frequency increases dramatically. These trends are shown in Figure 3.1. The terms upper and lower shelf refer to droplet frequency.

Lesnewich defined the transition current as the median current between the upper and lower shelves. While operating at currents along the lower shelf, the dominating mode of metal transfer is globular. During higher current operation, such as the ones found along the upper shelf, the mode of transfer begins with projected spray and shifts to streaming spray with increasing current. Ushio et al. [9] performed extensive testing on metal transfer modes with a variety of shielding gas compositions and currents. Figure 3.2 is a map of various transfer modes at different currents and compositions. Swirling, or rotating spray transfer can be achieved with even higher operating currents than spray transfer. However this mode is erratic and unstable, creating welds of poor quality. The transition event marks the shift of metal transfer mode from globular to spray. During operation, no one metal transfer mode is certain. One mode may dominate, but due to the dynamics of the welding process, instances of other metal transfer modes will occur.

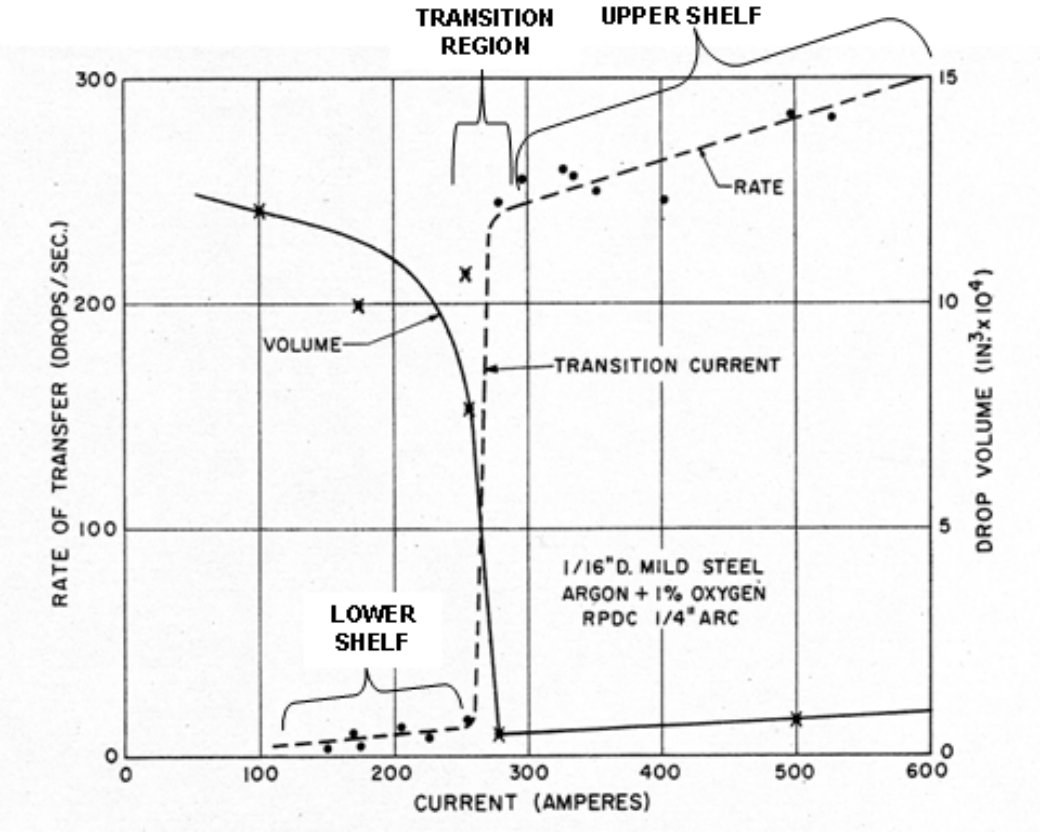

Figure 3.1. Effect of current on droplet detachment frequency and drop volume in an argon-rich atmosphere. [25]

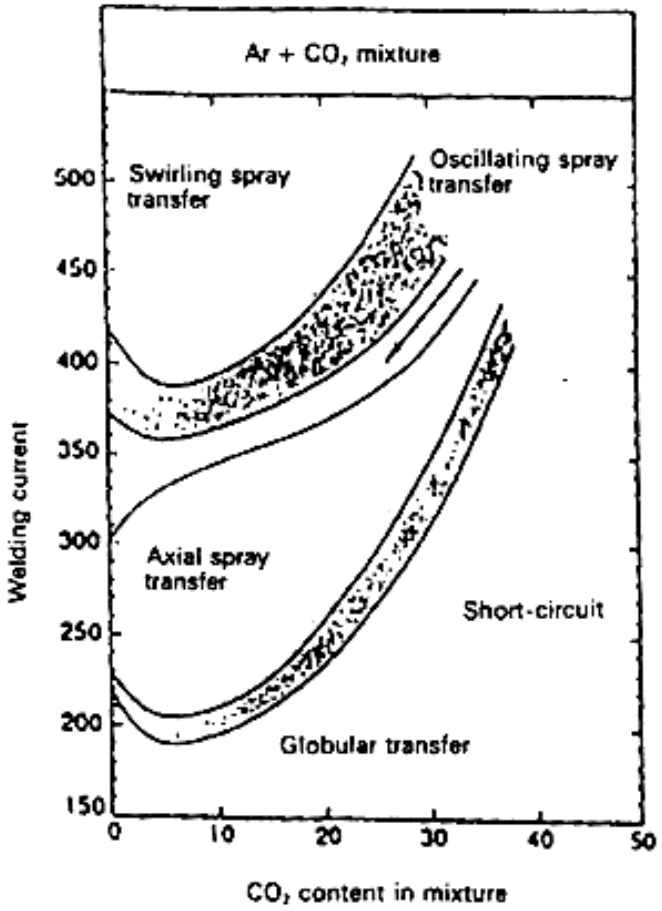

Figure 3.2. The different metal transfer modes for a given current and shielding gas composition for 0.045 in. (1.2mm) electrodes and CTWD of 1.0 in (25 mm) [9]

Further analysis by other researchers reveals several other characteristic changes that coincide with the shift of transfer mode. These changes include geometric relationships between the droplets and the electrode, the electrode and the arc and the resulting shape of the electrode tip. By studying these changes, criteria can be established to define transition in a number of ways. Not only does this make identifying the transition region easier, but also it exposes a relationship between observations that help characterize the operation of the system.

3.1.2. Droplet Diameter as a function of Electrode Diameter

The traditional method of distinguishing between globular and spray transfer relates the droplet diameter to the electrode diameter [26]. Globular mode is defined as the droplet having a diameter that is greater than the electrode diameter. Spray mode is defined as the droplet having a diameter that is less than the diameter of the electrode.

3.1.3. Arc Attachment Point

A second characteristic change that occurs in the transition region is the shift of the arc attachment point. Through analysis of Lorentz forces, Amson [19] determined that the angle between the center of the droplet and the arc attachment point has a large influence on the magnitude and direction of the pinch force. This work was later revisited by Kim and Eagar [18], whose calculations support Amson's [19] and are shown in Figure 3.3. Plotted on the ordinate is F_2, the factor defining the magnitude and direction of the pinch force. F_2 is shown as a function of the angle theta, which is defined as the angle between the center of the droplet and the upper attachment point of the arc.

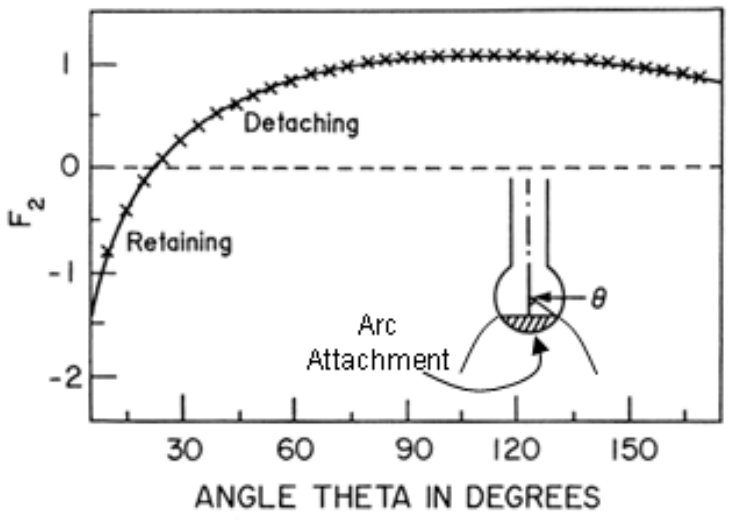

Figure 3.3. Variation of F_2, which determines the pinch force and direction, with the angle of arc attachment, θ. [18]

This angle is directly related to the area of the anode spot, which is represented as the shaded region in Figure 3.3. Thus, as the area of the anode spot increases, the angle θ will increase as well.

Quantitative experimental values of anode spot area are not known due to the difficulties associated with their measurements. However, qualitative observations made by researchers [27-29] are in good agreement with the models presented above. Small values of θ, which correspond with small anode spot areas, tend to produce larger droplets, consistent with a retaining force. In this case, droplets are able to grow to large sizes and globular mode is dominant. As current increases, anode spot area increases as well. The angle θ increases to a point at which the pinch force becomes positive and assists with droplet detachment. In this work, it is assumed that current density is a function of shielding gas composition and remains constant for a given composition [20, 29-32]; therefore, an increase in current will result in an increase of anode spot area. Figure 3.4 shows that increasing current changes the transfer mode from globular to spray. The characteristic change that occurs at the interface between the electrode and the arc (arc envelope) has a large effect on transfer.

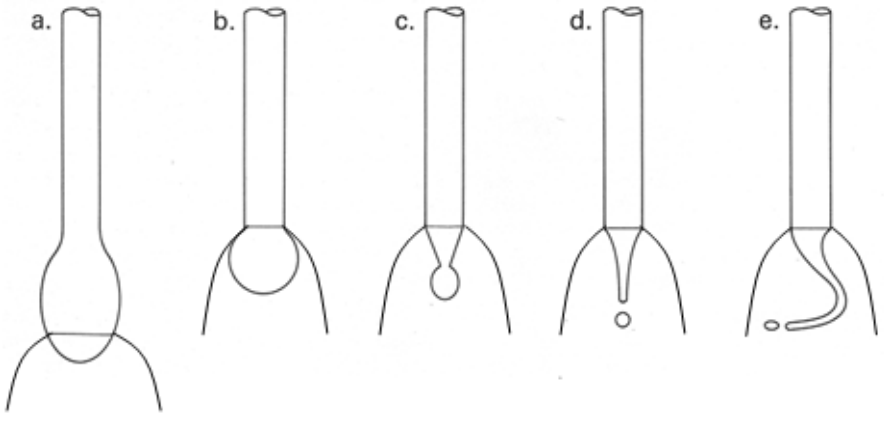

Figure 3.4. The effect of current on transfer modes. From left to right, current is increasing. [11]

3.1.4. Shape of the Electrode

One final characteristic change associated with the transition region is the geometric shape of the electrode in the vicinity of the arc. During globular mode, large spheres form and detach at a rate typically slower than 100 droplets per second. As current is increased and transition into spray occurs, a taper is formed on the end of the electrode, as shown in Figure 3.4c, d and e.

3.2. Carbon Dioxide in GMA Welding

Carbon dioxide is more widely available and less expensive than argon throughout the world. These cost savings for welding were identified as early as 1956 when Rothschild [3] reported that CO_2 shielded arc welding should be investigated by anyone involved in joining mild steel. However, changing the composition of the shielding gas affects several other characteristics of the welding process.

The following section will include the changes associated with CO_2 shielding, the theories used to explain these changes, as well as previous research made with CO_2. This will provide a background to the approach used in the present study, which will be explained in Chapter 4.

3.2.1. Effect of Carbon Dioxide on Metal Transfer

As CO_2 is added to argon, the transition current increases, as shown in Figure 3.5. This shift is apparent up to 25% CO_2, where the process becomes unstable and globular repelled transfer becomes the dominant mode of metal transfer at all currents. The transition to the spray mode has not been observed even with currents in excess of 1000 Amperes when using pure CO_2 as the shielding gas.

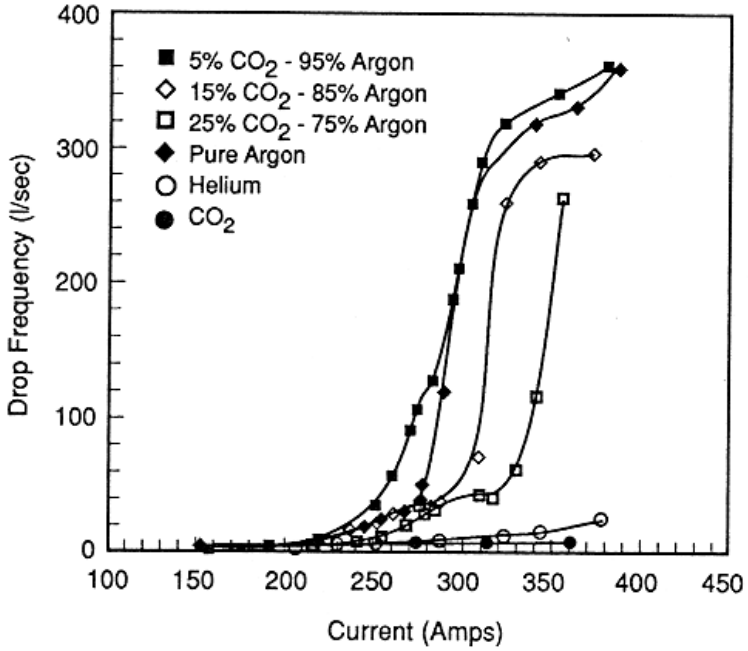

Figure 3.5. Effect of shielding gas composition on transition region. Increasing amounts of CO_2 increase transition current until no transition is observed. [27]

Repelled transfer is typically avoided because of the erratic motion of the arc, the high amount of spatter produced, and the poor weld quality [1-3, 11, 27, 33-35]. Traditionally, using short-circuiting transfer solved these problems; however, by doing this, a large decrease in deposition rate occurs. It is often beneficial to use higher-priced argon in the shielding gas to operate in spray transfer and have an overall reduction in cost due to the higher deposition rates.

3.2.2. Effects of CO_2 on the Arc

As increasing amounts of CO_2 are added to an argon atmosphere, the arc becomes increasingly constricted, the pressure exerted on the droplet from the plasma increases, and the current density in the anode spot increases [20, 30-32]. These changes are attributed to the large differences in thermodynamic properties, mainly thermal conductivity, between argon and carbon dioxide at temperatures seen in the welding arc. Figure 3.6 shows how thermal conductivity varies with temperature. The dissociation and ionization that occurs with CO_2 molecules corresponds with the many peaks that are evident. Argon experiences only ionization at elevated temperatures. Similar changes in

arc characteristics occur with additions of nitrogen, oxygen and hydrogen. The plasma properties have a marked influence on the EM forces acting on the droplets which is clear from the observation that the arc attachment at the anode tip is wide when the plasma gas is argon and becomes narrow with increasing amounts of CO_2 [27]. Mechev et al. [30] showed through calculations that arcs established in CO_2 are more concentrated sources of heat on the droplet than those operating in argon because the power and dynamic processes that occur in CO_2 are concentrated within a narrower region when compared to argon.

Nemchinsky [20] modeled the current conduction in the near-anode plasma layer and compared current distributions between argon, helium, and molecular gases (CO_2). He showed that the anode layer covers less area in CO_2 than in argon for the same current. These observations and calculations support the assumption that current density at the anode tip is highly dependent on the shielding gas used and increases with CO_2 concentration.

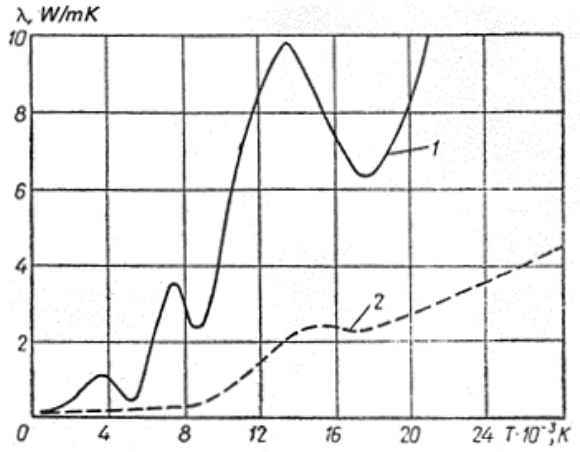

Figure 3.6. Thermal conductivities for carbon dioxide (1) and argon (2). [30]

Mendez et al. [36] used Order-of-Magnitude Scaling (OMS) to estimate the plasma pressure in the near-cathode region for GTAW.

The maximum pressure estimation is given as:

$$\hat{P}_S = \frac{1}{2}\mu_0 R_C^2 J_c^2 \qquad 3.1$$

where μ_0 is the permittivity of free space, R_c is the cathode spot radius, and J_c is the current density. Even though these calculations were based on GTAW, similar pressure distributions will be found near the anode in GMA welding. As current density increases, the maximum pressure of the plasma increases as well. When pressures become large enough with increasing amounts of CO_2, the resulting force on the droplet may become large enough to suspend the droplet or even repel the droplet away from the arc.

3.3. Attempts at Overcoming the Problems Associated with CO_2

Many attempts have been made throughout the past several decades to produce spray transfer with CO_2 despite the well-known challenges that exist. In the 1950s, a method was developed by the Air Reduction Co. (AIRCO) that enabled spray-like transfer using CO_2 shielding gas[1, 2]. The researchers concluded that spray transfer is impossible when the path of welding current at the tip of the electrode is confined to a small high-current density area. They postulated that by having a negative polarity in the electrode and adding emissive agents to the surface of the electrode they could control the current density at the tip of the wire. The method involved covering the electrode with extremely dilute coatings of alkali and rare-earth metals. It was found that spray transfer was achieved in pure CO_2 with compounds of sodium, potassium or rubidium added to compounds of cesium in equal atomic concentrations then applied as a coating to electrodes containing deoxidizing agents (Si and Mn). Negative polarity usually is not used during GMA welding because it produces an unstable arc, much spatter, and poor weld quality. However, the coated electrodes operated in spray transfer, with minimal spatter and good weld quality.

The reason for accomplishing spray transfer in these conditions has been attributed to changes in thermionic emissivity. During traditional GMA welding, operating with direct current electrode positive (DCEP), the workpiece is the electron emitter (cathode) and the wire electrode is the electron absorber (anode). Electron emission and electron absorption are fundamentally different. The emission of electrons from the coated cathode is due to thermionic emission, which is dependent on the work function and temperature of the metal. The coatings have a much higher thermionic emissivity than the electrode, and when used in conjunction with DCEP, reduce the work function of the electrode. The electrode is then able to emit electrons from a larger area, changing the current density on the electrode tip, and changing the mode of metal transfer.

Beginning in the 1960s, Needham and Carter [37] began experimenting with pulsed current power supplies in an attempt to overcome the limitations of constant voltage/current. One of the benefits of using pulsing current is regulation of the arc forces. Having the ability to change operating current in milliseconds is the same as changing the EM forces in the same amount of time. The basic principle is to detach the droplet with a large current pulse, then reduce the current to melt the wire, and then repeat this process. These results showed that it is possible to have better quality welds made at larger deposition rates in CO_2 when using the pulsing current under suitable conditions. Nonetheless, this new technology was unable to surpass the quality of welds made with argon-based gases.

With the computer age, the past several decades has seen a large increase in power supply technology. In the mid 1980s, Matsuda et al. [38] used an adjustable rectangular-wave pulse machine to create welds in CO_2 that created ~20% the spatter of non-pulsed CO_2 welding. Using 0.045 in. diameter wire, mean current of 250A and pulsing frequencies of about 38Hz, the transfer mechanism was observed using high-speed cinematography and shown schematically in Figure 3.7. It is evident during the

high current pulse the constricted CO_2 arc acts upon the droplet causing a large distortion, while the EM pinch force creates a necked region in the wire.

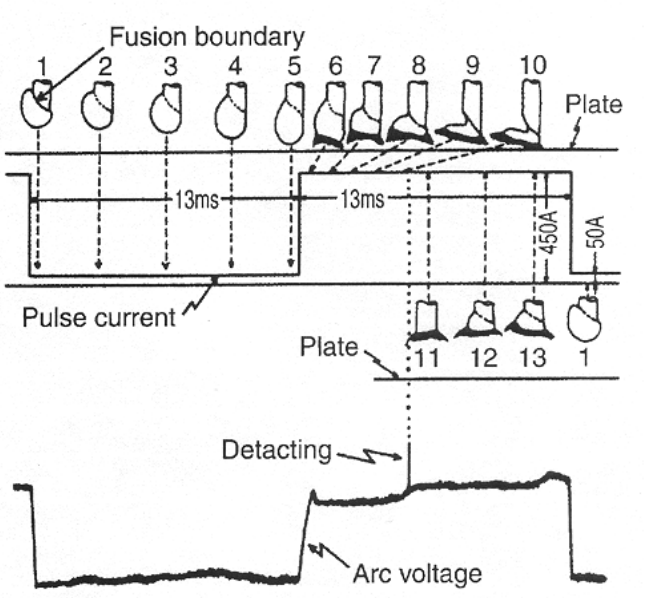

Figure 3.7. Example of pulsed current CO_2 welding. Droplet transfer is shown in correlation to the pulsing events. Black areas represent the arc. [38]

Even with these advances, spray transfer has not been accomplished for CO_2, and free flight transfer in CO_2 using pulsed power sources still produces more spatter, poor bead appearance, and erratic arc behavior when compared to welds made in an argon-rich atmosphere.

Current state-of-the-art processes for GMA welding use advanced short-circuiting metal transfer with CO_2. Sophisticated computer program control of welding parameters enables waveforms never before used in GMA welding. The technology is described in detail by Cuiuri et al.[34], where the droplet is formed with a large current pulse, dipped into the weld pool, and detached by surface tension due to the weld pool. The two largest power supply manufacturers in the United States both have their versions of this system: Miller Electric has Regulated Metal Deposition (RMD^{TM}) and Lincoln Electric developed Surface Tension Transfer (STT). Deposition rates are approaching those of free-flight

transfer, but limiting factors such as stubbing and arc length changes become prominent at high wire feed speeds. A sophisticated reversing wire feed system was implemented to account for these problems; however, experimental results have not been published yet.

3.4. Summary

The transition region phenomenon is unique and has been shown to occur in GMA welding. Increasing current and feedrate to the transition current produces a sharp increase in droplet detachment frequency and decrease in droplet volume. Along with this, the arc envelopes the droplet, droplet diameter becomes smaller than electrode diameter, and the electrode forms a taper at the region of detachment. These characteristics have all been shown to be characteristic changes associated with the transition region.

The ability to achieve high deposition rates while using CO_2 shielding has been pursued for the last half-century through a variety of methods. Increasing the amount of CO_2 in the shielding gas has several drawbacks. They have been shown to include a constricted arc, an increase in plasma pressure and higher current densities on the electrode tip, all of which are related to repelled globular transfer.

By increasing the current densities through emissive coatings and regulating the arc forces with pulsed current power supplies, researchers have improved weld quality while keeping deposition rates high. However, many fabricators find it beneficial to use argon-based shielding gases due to the superior weld appearance and stable operation. Based on the observations made in previous research, a new approach is proposed that may permit spray transfer, as seen in argon, to occur in atmospheres containing more than 25% CO_2. This hypothesis is developed in the next chapter.

4. RESEARCH HYPOTHESIS

The goal of this research is to explore a process that has the advantages of spray transfer and the cost savings of CO_2. It has been shown in Chapter 1 that cost reductions can be realized using CO_2 in spray transfer. However, it was also shown above that CO_2 and spray are mutually exclusive. Despite extensive research efforts, the use of pure CO_2 GMA welding in high-production, high-quality applications has not found support in industry. By exploring the effects of wire diameters and shielding gas composition on metal transfer, we expect to expand the range of usable compositions.

The research hypothesis of this work is that spray transfer in CO_2 should be attainable by using small enough wires such that the anode spot completely envelopes the electrode tip.

4.1. Development of Hypothesis

One of the main assumptions in the formulation of this research hypothesis is that current density is mainly a function of shielding gas. The current density on the anode tip is the welding current per anode spot area. The anode spot area is the area where current is transferred from the plasma to the electrode. In this case, the properties of the plasma in the near-electrode region will dictate the area of the anode spot. Similar assumptions have been made by other researchers [18, 27, 31] for modeling of the GMA welding process. Figure 4.1 shows a schematic of increasing current in an argon-rich atmosphere from left to right. The current density remains constant because there are no changes in the composition of the shielding gas, so any changes in current will lead to an increase in anode spot area. There is a point at which the anode spot area becomes large enough to

envelope the droplet and transition. This model can explain the globular to spray transition as presented in Section 3.1.1.

Qualitative experimental observations and theoretical calculations show that CO_2 increases current density at the anode tip as illustrated in Figure 4.2. From left to right, the amount of CO_2 in the shielding gas is increasing. For a given current, increasing the amount of CO_2 decreases the anode spot area. In effect, this pushes the arc attachment point from above the droplet to below it, reverting from spray transfer to globular. Arc constriction also occurs and globular droplets form.

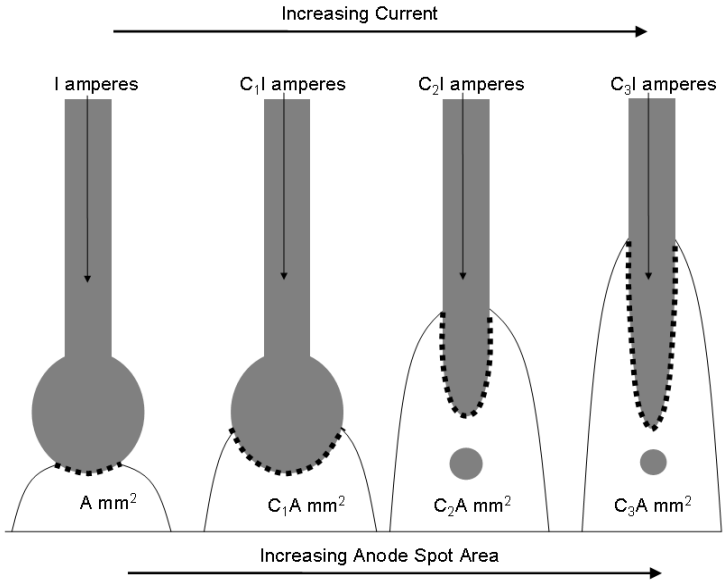

- $1<C_1<C_2<C_3$
- Current density remains constant
- Transfer mode changes with current

Figure 4.1. A simplified hypothetical model showing the effects of increased welding current in argon. Current density remains constant at I/A(Amperes/mm^2) as the arc climbs over the droplet. Transition occurs when the arc envelopes the droplet.

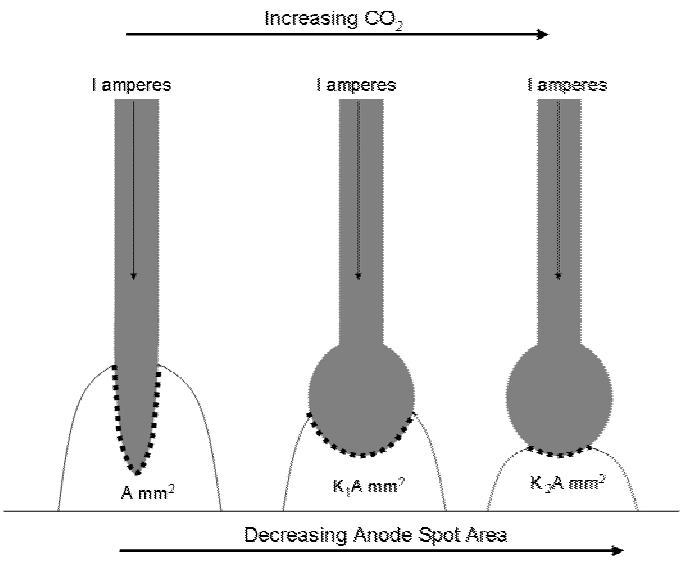

- $1>K_1>K_2$
- Current density increases with CO_2
- Transfer mode changes with anode spot area

Figure 4.2. A schematic of the proposed effects of CO_2 on current density and metal transfer. Anode spot area decreases with increasing CO_2.

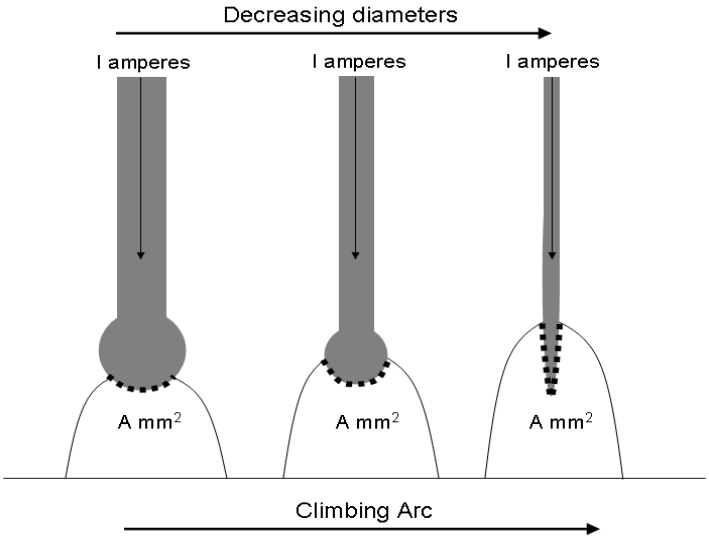

- Current density remains constant
- Transfer mode changes with arc attachment

Figure 4.3. Schematic showing the anticipated effects of decreasing wire diameter. Current densities remain constant, but a change in transfer mode occurs due to arc attachment point.

Published GMA welding research often uses 0.045 in. (1.2mm) or larger diameter wire. By physically decreasing the minimum diameter of the electrodes, it is expected that the arc will compensate by covering more of the droplet, as shown in Figure 4.3. From left to right, the diameter of the electrode is decreasing. Assuming the shielding gas remains constant and current density does not change, it is hypothesized that the arc attachment point will climb up the electrode.

To offset the constricted arc that accompanies high CO_2 concentrations, thinner wire diameters will be used. It is expected that the arc will be forced to climb the electrode to maintain a constant current density. As the arc climbs over the droplet, transition will occur and spray transfer will be the dominant metal transfer mode.

4.2. Summary

The transition from globular to spray transfer occurs quite suddenly in argon and has many characteristic features. These characteristics include the droplet diameters becoming smaller than the electrode diameter, the arc attachment moving above the droplet onto the electrode and tapering of the tip of the electrode. Additions of CO2 constrict the arc, leading to high current densities. With electrodes of 0.045 in. diameter and greater, these high current densities lead to large plasma forces and create repelled globular transfer. Our hypothesis states that if small enough electrodes are used, the arc will be forced up and over the droplets, leading to a transition into spray. The next section will cover the details of the experimental setup.

5. EXPERIMENTAL METHOD

This chapter will present the setup and procedure that is used for the experimental analysis. It is divided into two sections: the experimental apparatus and the experimental procedure used in this research.

5.1. Experimental Apparatus

The main components of any gas-metal-arc welding system are the power source, the wire feeder, and the welding torch. The system used in this research includes all of these components as well as many sub-system components that allow precise measurement and control of welding variables. This section explains each component, how it works, and its importance to the overall system. Figure 5.1 shows the entire system with all pertinent components labeled.

5.1.1. The Power Source

The power source used in this research is a Miller Maxtron 450 CC/CV machine. It is a commercially available system that is widely used in industry, and any improvements that are discovered can be directly implemented in real-world applications. The configuration of the power supply is such that direct current/constant voltage is used. No pulsing current or waveform programming is implemented in the experiments, due to the increased complexity. No modifications were made to the power source that would change its output characteristics. During constant voltage (CV) operation, the output of the machine creates a self regulating arc that is necessary for stable operation when used in conjunction with a constant-speed wire feeder. The characteristics of this output are

shown in Figure 5.2. A slight change in arc voltage (arc length) gives rise to substantial changes in current. This response can compensate for variations in the contact tip to workpiece distance, which may occur during normal manual welding operations. The initial arc length is set by the operator by adjusting the voltage at the power source. If the arc length decreases (voltage decreases) during operation, perhaps the operator was to shift or the workpiece moves, the machine will increase current (electrode burnoff) to increase arc length to the original set value. If arc length (arc voltage) was to increase from the set value, the machine would respond by decreasing current (electrode burnoff) to return to the set voltage value. This self-regulating feature of GMA welding makes the process very stable and the resulting welds are of high quality.

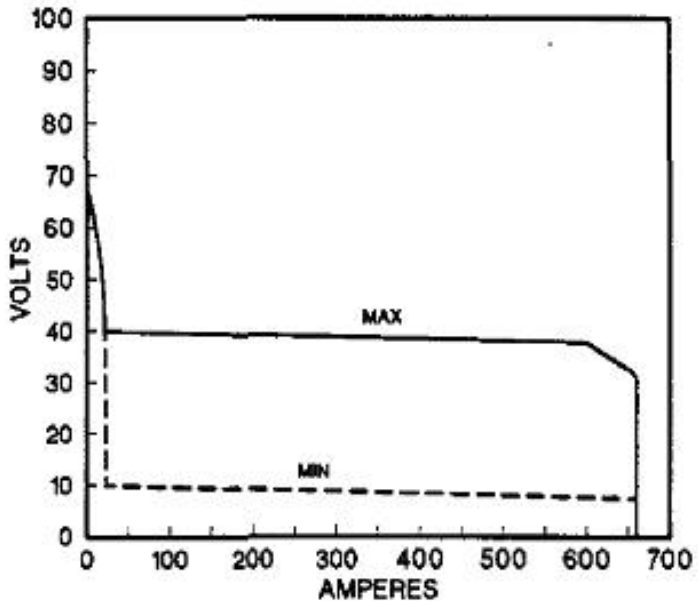

Figure 5.2. The characteristic volt-ampere curves for the Miller Maxtron 450. The minimum and maximum output capabilities are shown for the power source. Curves for other setting fall between the curves shown. [39]

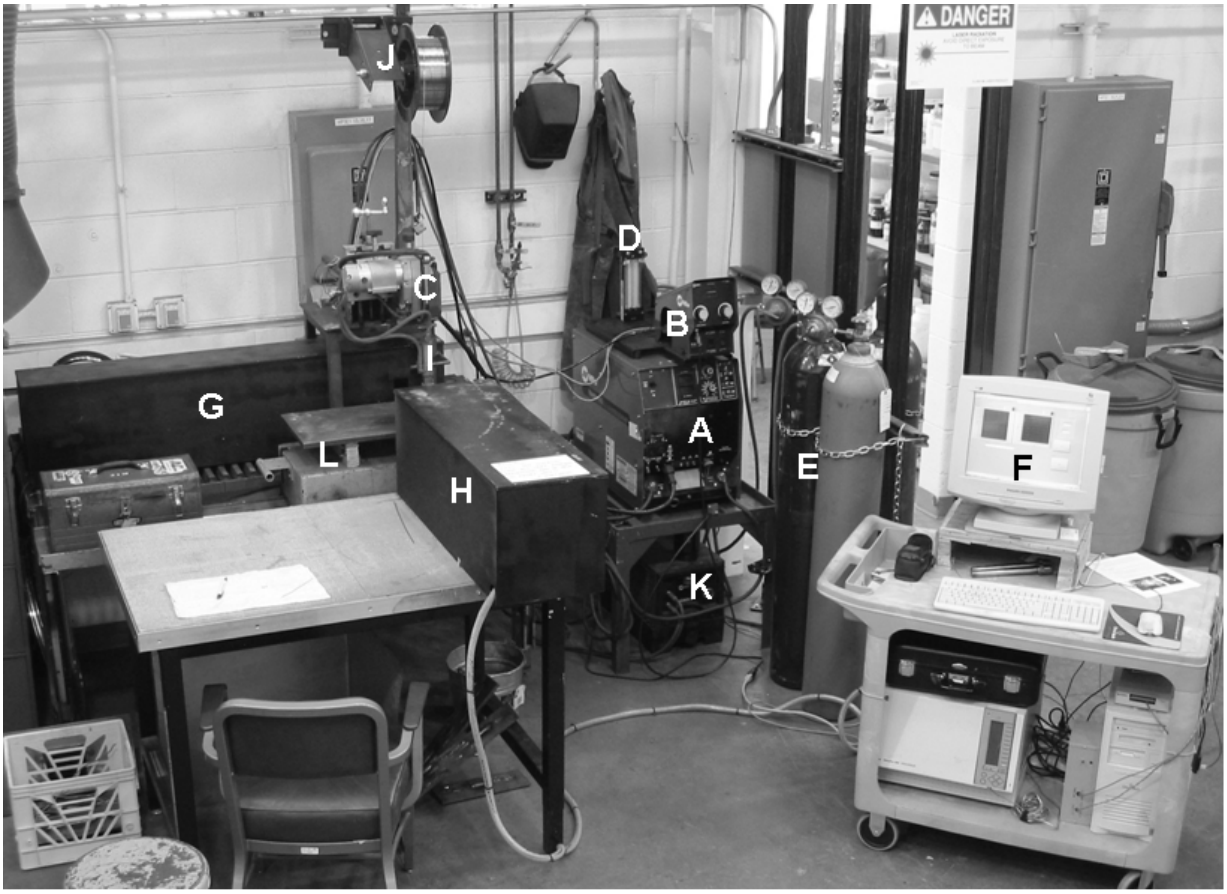

A – Power Supply
B – Control Interface
C – Wire Drive Assembly
D – Gas Mixer
E – Gas Cylinders
F – Data Acquisition
G – Laser
H – High Speed Camera
I – Welding Torch
J – Electrode Spool
K – Water Cooler
L – Moving Workpiece

Figure 5.1. The entire experimental setup.

5.1.2. Constant Speed Wire Feeder

The second main component of the system is the wire feeder. Several modifications were made to the unit to improve the performance during this research. The wire feeder used in the research was donated by Miller Electric Manufacturing Company. It is a model S70 with the high speed motor option, enabling wire feed rates up to 1443ipm. The as-received unit is shown in Figure 5.3.

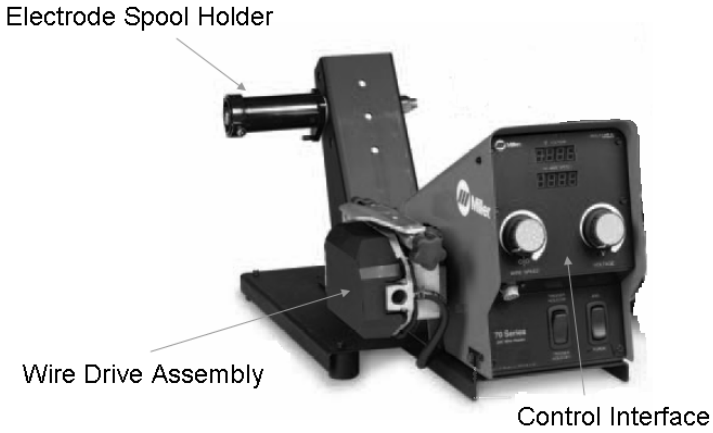

Figure 5.3. A picture of the as-received wire feeding unit, which is a Miller S-70 model with high-speed motor option [40].

t was modified so that it could feed the 0.016 in. wire. The changes are shown in Figure 5.4. The wire drive assembly was removed from the case and relocated closer to the contact tip. The thin wire is very susceptible to buckling. By decreasing the distance between the contact tip and the drive rolls, there is less tendency to buckle. This distance was reduced from 72 to 8 inches through the modifications. Along with this improvement, the electrode spool holder needed to be relocated to ensure a straight path from the spool to the ingress of the wire drive assembly.

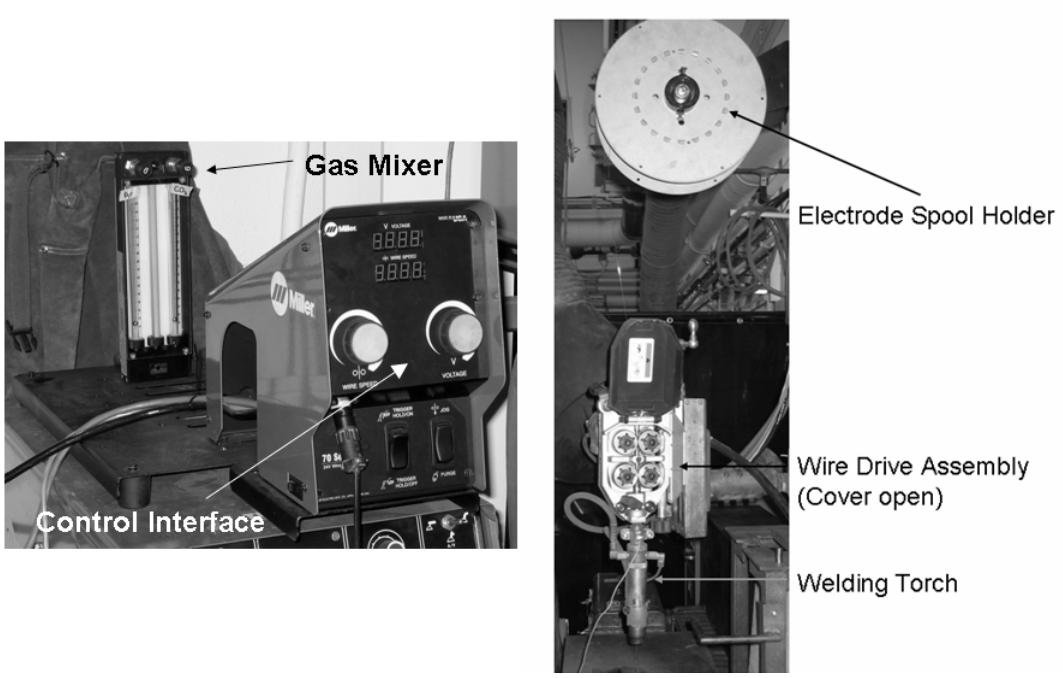

Figure 5.4. A detailed view of the modified wire feeding unit. The distance from the end drive rolls to the welding torch has been minimized to prevent buckling and allow smooth feeding of small diameter electrodes.

5.1.3. Welding Torch and Contact Tips

Using small diameter wires and high wire feed speeds presents many unique challenges. For instance, the electrode becomes much more susceptible to buckling as wire diameters decrease. This problem can be addressed by minimizing the distance between the drive rolls and the contact tip. Another challenge that needs to be dealt with is the contact tip itself. Currently, commercially produced contact tips, similar to the one shown in Figure 5.5, accommodate wires as small as 0.023 in. diameter. The smallest diameter that will be used in this research is 0.016 in. Either customs tips of the same design need to be fabricated or a contact tip of a different design will need to be fabricated.

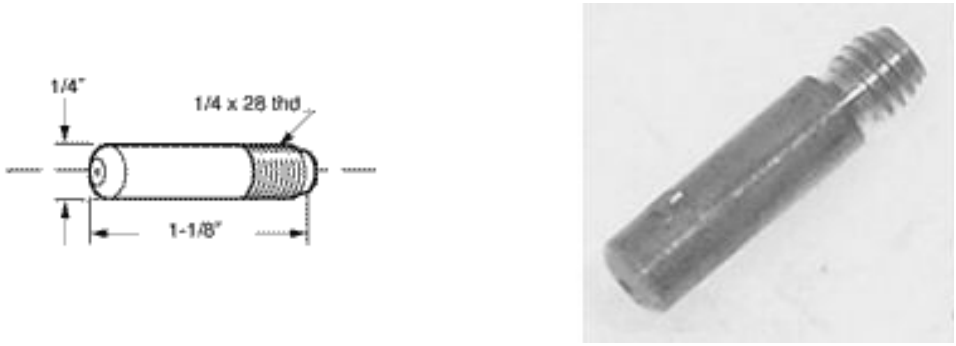

Figure 5.5. A schematic drawing (left) and a picture (right) of a commercially available conventional tube contact tip sold today (Model GA-17C). The smallest wire size that can be used is 0.023 in. diameter. In this study, 0.016 in. diameter wire will be tested, creating a need for a custom contact tip.

The welding torch used in the research was a Miller type GW-60A. It is shown in Figure 5.4. This torch is water cooled and rated up to 500A. An adapter was fabricated to allow the use of smaller contact tips: commercially produced Miller type GA-17C. 0.045 in., 0.035 in., and 0.023 in. sizes are available in this configuration. These contact tips are common welding parts and were readily available at the local welding shop, General Air Service and Supply.

Despite an extensive search, no commercially available tips were found for the smallest wire diameter, 0.016 in. The first attempt to fabricate contact tips to use with the small wire involved using the same tubular design as larger commercially produced contact tips. ¼ in. copper round bar stock was machined to the same external dimensions as the GA-17C. Then, a 0.016 in. hole was drilled through the center of the rod. Fabrication of these tubes was extremely difficult and tedious. A special high-speed drill was needed for the operation. Twenty tips of this design were made and welding commenced.

Burnback, which is an unfavorable event that occurs when the electrode recedes into the contact tip and causes gross melting, were common. The mechanism of burnback is explained by the following:

- The arc is initially maintained between the workpiece and the electrode
- Through unstable welding conditions the stick-out distance becomes substantially decreased. These conditions can be erratic arc, stubbing, transients, or changes in position of current transfer in the contact tip.
- The heat from the arc melts the contact tip.
- When the arc is extinguished, the molten copper solidifies and entraps the electrode, rendering it useless.

The small dimensions of the holes (0.016 in.) that are used in the traditional contact tip made them extremely sensitive to burnback, occurring at a rate much higher than what was experienced with the larger wires. Commercially produced contact tips that were used with the larger wires could be used for as many as 50 experimental runs. Twelve experiments were performed before all of the custom manufactured contact tips were destroyed. A week of machining was burnt up in less than an hour of testing. A new contact tip design was needed.

The newly designed contact tip is shown in Figure 5.6. It incorporates features that aid in small diameter electrode welding. One of the problems with the traditional tubular contact tip design is the uncertainty in the exact position of current transfer between the contact tip and the electrode. Waszink and Van Den Heuvel have estimated this point to shift as much as 1.25 mm during welding operation [41]. If contact points vary, so does the effective electrode extension. To prevent this shifting from happening, the current transfer point was precisely controlled to the intersection of the perpendicular wires, one being U-wire on the contact tip and the other is the electrode wire. Everywhere else, the electrode is insulated from the welding current, assuring current transfer occurs at that point. The electrical insulation is provided by a thin alumina tube

that sheaths the electrode from the contact tip. This design is needed as wire diameters become smaller and process stability becomes more sensitive to small changes in welding parameters.

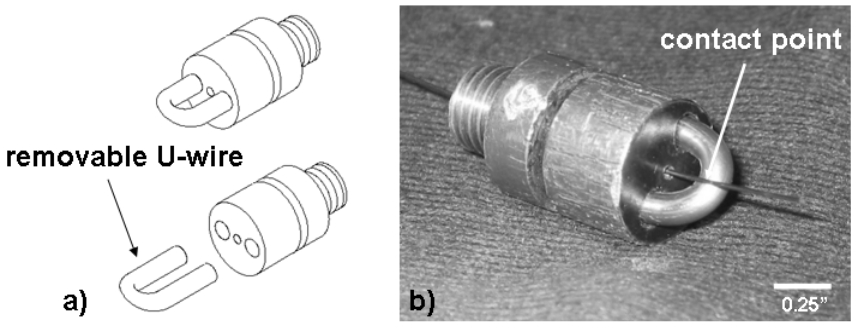

Figure 5.6. The schematic drawing of the newly designed contact tip (a) and the fabricated part (b) is shown. The electrical contact point is restricted to the point shown.

A second key design element of the contact tip is an improved failure mechanism. In the new design, the U-wire acts as a sacrificial anode if the arc climbs burns back the electrode sufficiently. Instead of the arc melting back the electrode into the hole, the arc is transferred to the copper U-wire and melts it instead. By the time burnback is detected, the arc can be extinguished before gross melting of the contact tip occurs. The U-tip can be replaced and welding can resume with minimum downtime. The consumable U-tip is simply a copper wire bent into a U shape. Tools needed consist of wire cutters and pliers. No precision machining needs to be done. This design element decreased the burnback frequency and increased the process stability. It has a patent pending [42]

5.1.4. Shielding Gas Control

An Omega gas proportioning rotameter Model FL-2GP-40ST-40ST was used for varying the composition of the shielding gas. A calibrated flowchart was supplied from the manufacturer for infinitely adjustable binary gas blends of CO_2 and argon. Constant

flow rates of 40 CFH were used throughout the entire study. The gas mixer was received from the factory calibrated with an accuracy of ±2% in composition.

5.1.5. Automated Welding Setup

The initial automated welding configuration consisted of stationary workpiece with a moving torch. This type of setup allows easy arrangement of the workpiece and torch in relation to each other so that a variety of positions and geometries can be utilized. The drawback to this system, however, is that arc imaging is extremely difficult because the arc is constantly moving. One of the main objectives of this research is to image and study the arc, so reversing the roles would of the torch and workpiece would make imaging much easier. In addition to making imaging easier, the modified torch was much heavier than the previous. These two reasons made it sensible to fix the position of the torch and have the workpiece move. A stationary torch-moving workpiece apparatus was constructed. The results are shown in the figures above.

5.1.6. Current and Voltage Data Acquisition

Determining the metal transfer mode is critical for this investigation. Several methods exist that have been used by researchers. Adam and Siewert [5] used arc voltage and current analysis to determine metal transfer modes. Many other researchers have used similar methods for determining metal transfer modes and characteristics.[8, 43, 44] It is relatively simple to measure the droplet transfer rate by sampling the voltage and current during the welding process and examining the oscillations in these signals.

The current was measured with a LEM HTA 600-S (current transducer), which has a current range between 0 and 600Amperes. A LEM LV25-P (voltage transducer) was used for voltage sampling and was capable of sampling between 0 and 100 Volts. These were connected to a signal processing box, fabricated in-house by Scott Pawelka. The outputs of the box ranged from 0 to 10 Volts. The voltage channel was scaled down by a factor of ten, meaning that a reading of 100 Volts at the probe would output 10 Volts. Current output was 6.67mV per 1 Ampere of welding current. The outputs of the

signal processing box were connected to a National Instruments SCB-68 shielded connector block which was interfaced to a computer containing a National Instruments PCI-6220 data acquisition card. The software used was National Instruments Labview 7.0. Data was sampled at 5 kHz. Welding current values for a given point are an average for the entire sampling time (25k samples). The accuracy for a given sample is ±5A.

5.1.7. Metal Transfer Imaging

The study of metal transfer is difficult given the nature of the environment. Temperatures in the arc regularly exceed 10,000K and the intensity of arc light is more than the sun. Nonetheless, visual changes that occur during welding are important to the process operation. Another method of determining the metal transfer mode involves arc imaging.

Preliminary attempts at imaging the arc were made with a Canon S30 digital camera. A characteristic photograph is shown in Figure 5.7. This image was taken with an arc welding filter of shade 10. The shutter speed was set at 1/750 of a second and the welding parameters were 0.035 in. diameter electrode operating in spray transfer in an argon atmosphere with 30V and 250A. The arc is well defined; however, that is the overwhelming feature of all of these digital photographs. Droplets cannot be distinguished and even if they were apparent, the droplet rates cannot be computed because it represents a single point in time, however, it does show two characteristics of spray transfer: tapering of the electrode and arc enveloping the electrode. To distinguish metal droplets within the arc, a laser shadowgraph system was implemented.

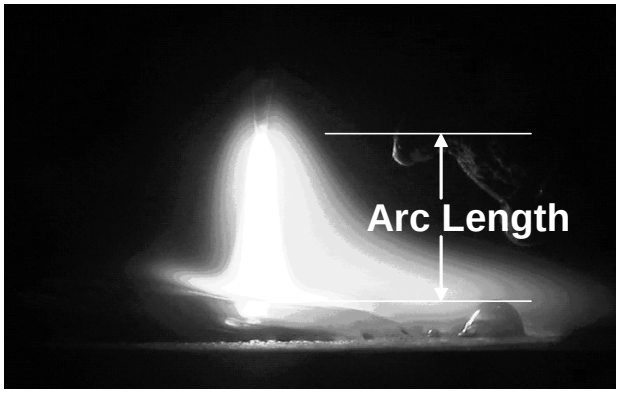

Figure 5.7. A digital photograph taken of the welding arc. The welding parameters were 0.035 in. diameter electrode, 100% argon, 30 Volts and 250 Amperes. Metal transfer mode is streaming spray.

The principle of a laser shadow-graph system is relatively simple. It is very similar to making shadow puppets from behind a curtain. In this setup, a laser is used as the light source and the metal droplets are what project the shadows onto the surface. By recording the shadows with a high-speed camera, the dynamic process of droplet detachment can be seen. The system was loaned by the National Institute of Standards and Technology (NIST) in Boulder, CO. The setup is very similar to the one used by Allemand [6]. Figure 5.8 shows a schematic of the setup. All components were manufactured by Melles-Griot, except the reflecting mirror. The laser source is a Helium-Neon laser with a maximum output of 30 mW at a wavelength of 632.8 nm. The beam was then passed through a model 09 LSF 011 spatial filter and then a 09 LCM 013 collimator. Beam intensity and diameter was adjustable with these components. A Newport HeNe laser line dielectric mirror mounted to an adjustable mirror mount allowed precise aiming of the beam. The arc light was filtered through a Melles-Griot 03 FIL 022 bandpass interference filter. The shadow image was projected onto a piece of frosted glass and filmed with high-speed video. Figure 5.9 is a still image of the video taken during the welding process. The dark areas are the shadows projected onto the screen, whereas the light areas are laser light that passes through unimpeded.

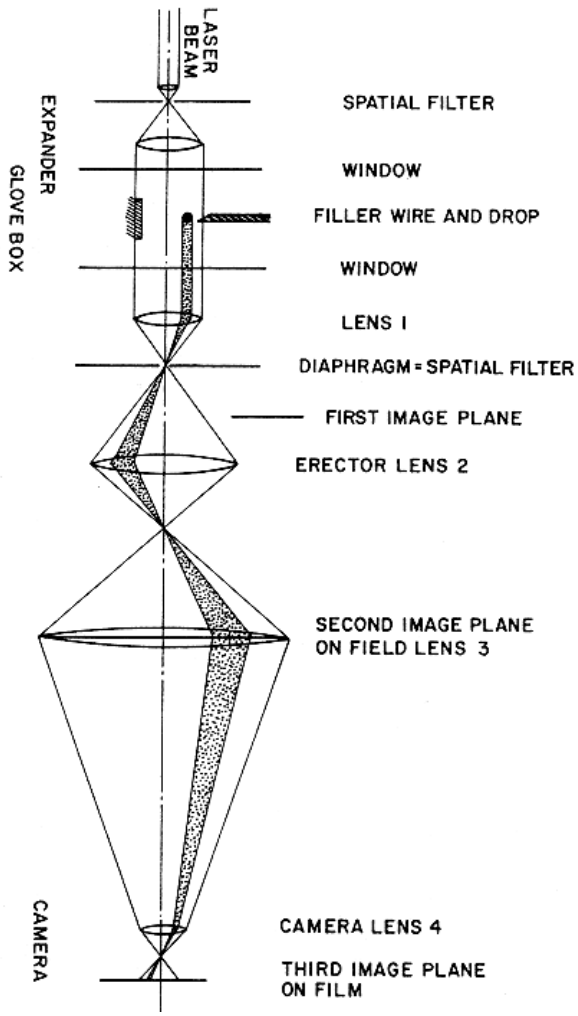

Figure 5.8. A representation of the laser shadow-graph system that is used in this research. [6]

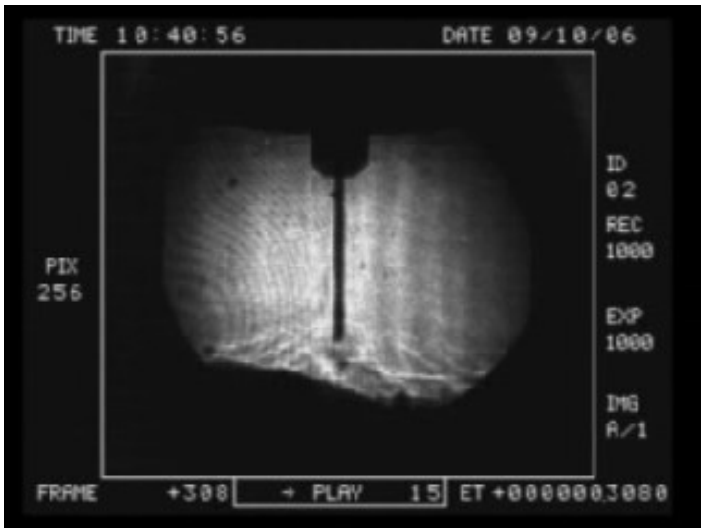

Figure 5.9. A screen shot of the high-speed video shadow-graph. The contact tip shadow is clearly visible at the top of the screen, with the electrode shown in the middle.

A Kodak EktaPro EM digital high-speed camera was used to record the welding process. An Olympus 50mm lens mounted to a 12mm extension tube and a C adapter provided the best images. The videos were recorded at 3000 frames per second.

The video system was interfaced to the computer through an ADS Technologies USBAV-709-EF to allow direct digital recording of the movies stored on the EktaPro processor.

5.1.8. Shielding Gas

The shielding gas used in the study was a binary mixture of industrially pure argon and CO_2. Industrially pure argon is 99.98% pure.

5.1.9. Material

The 0.045 in., 0.035 in. and 0.023 in. diameter electrodes were all classified as AWS ER70S-6. The classification of the 0.016 in. diameter electrode was AWS ER70S-

G and the chemical compositions are given in Table 5.1. Welds were made on 3/8 in. thick ASTM A36 structural bar steel.

Table 5.1 Electrode size, classification and chemical composition

Wire Diameter	AWS Classification	Composition (weight %)					
		C	Mn	Si	P	S	Cu
0.045"	ER70S-6	0.07 to 0.15	1.40 to 1.85	0.80 to 1.15	0.025	0.035	0.50
0.035"	ER70S-6						
0.023"	ER70S-6						
0.016"	ER70S-G	0.13	0.51	0.08	0.010	0.010	0.62

5.1.10. Arc Length Control

Figure 5.10 shows the apparatus used to control arc length. A tungsten indicator was placed in close proximity of the electrode. Prior to welding, the height can be adjusted for the desired arc length. Once the process is initiated, the voltage can be adjusted to the height of the indicator.

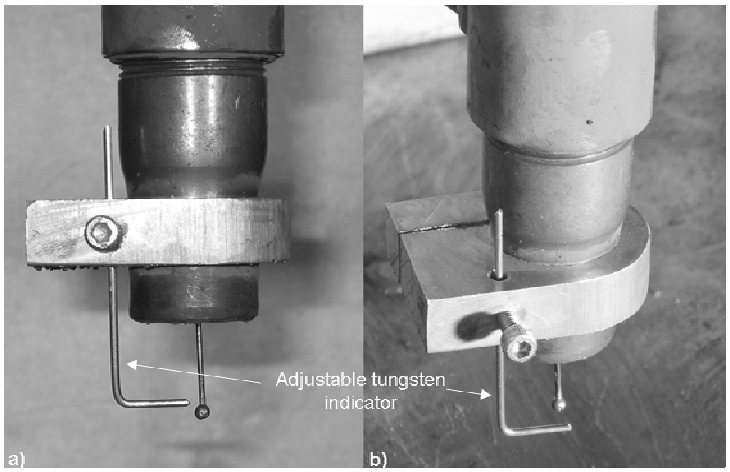

Figure 5.10. The apparatus that was fabricated to keep constant arc lengths. The tungsten indicator is able to withstand high temperatures and is adjustable to reference various arc lengths.

5.2. Experimental Test Method

The goals of the experiments was to classify the metal transfer modes with four different wire diameters and varying amounts of CO_2 in the shielding gas. Comparing the trends will show relationships between these variables.

The procedure for collecting data is described in this section. A brief overview of the process is given below:

- Pre-welding machine setup is necessary to ensure proper operation. This setup includes inspecting all cables, tubing, and junctions for leaks and unsafe conditions. Proper sample preparation is critical for repeatable results.
- Flame cut the bar stock to the required dimensions, grinding any slag or sharp edges and grit blasting the surface clean to remove any mill scale or oil is used to prepare the samples.
- Install the correct electrode onto the electrode spool, along with the corresponding drive rolls and contact tip. Failure to match the correct sizes will result in erratic feeding and unstable welding conditions.
- Turn system power on for the power supply, torch cooler and data acquisition computer, signal processing unit, high-speed camera and laser.
- Connect voltage and current sensors. To the signal processing box.
- Load the Labview 7.0 program that was made to acquire current and voltage signals.
- Adjust shielding gas mixture to desired composition, as well as the wire feed speed.
- Set contact tip to workpiece distance (CTWD).
- Initiate the welding process and adjust voltage to correspond with desired arc length. Wait for the process to stabilize before initiating data acquisition. In all welding processes, large transients in voltage and current exist at the initiation

and termination of the process. These transients do not represent what happens during the steady operation regime and should be avoided due to deleterious data.

- Once the process stabilizes, initiate the current and voltage acquisition and the high-speed video recording.
- Terminate sampling after five seconds.
- Terminate the welding process.

Each test will produce a single text file, as well as a video clip. The text file contains three columns, representing time, voltage, and current. Post-weld processing of this data was done in Mathcad, where the data was scaled to the actual operating values, graphed, and assessed with Fast Fourier Transform (FFT). Figure 5.11a shows a representative graph of the voltage and time output for a weld conducted with 90Ar-10CO_2 shielding gas mixture. This particular example is very periodic. Figure 5.11b represents the Fast Fourier Transform of the voltage signal, and it is apparent that the most common frequency is 340 Hz. It is clear that a distribution of frequencies exists. In most cases, the range of frequencies was limited to a 100 Hz window. For comparison, Figure 5.12 is the signal take from a weld made in 70Ar-30CO_2 atmosphere. The signal is erratic and leads to uncertain values in the FFT. Further clarification of the exact transfer mechanism was determined by using laser shadowgraph techniques.

The most difficult variable to measure was the droplet detachment frequency. Unlike current and voltage, it cannot be directly measured. Three different types of analysis were used to determine this frequency: FFT of voltage, droplet counting in video, and peak counting of voltage. Previous analyses by researchers support all these methods for determining droplet frequency. Once the frequency is known, droplet volumes and diameter can be calculated. Comparing the measured frequencies from the different data sources, the error in droplet frequency was calculated. Droplet detachment frequency differences between high-speed video analysis and voltage signal analysis did not exceed ten percent at the maximum values. This error coincides with other researchers using similar methods [18, 45].

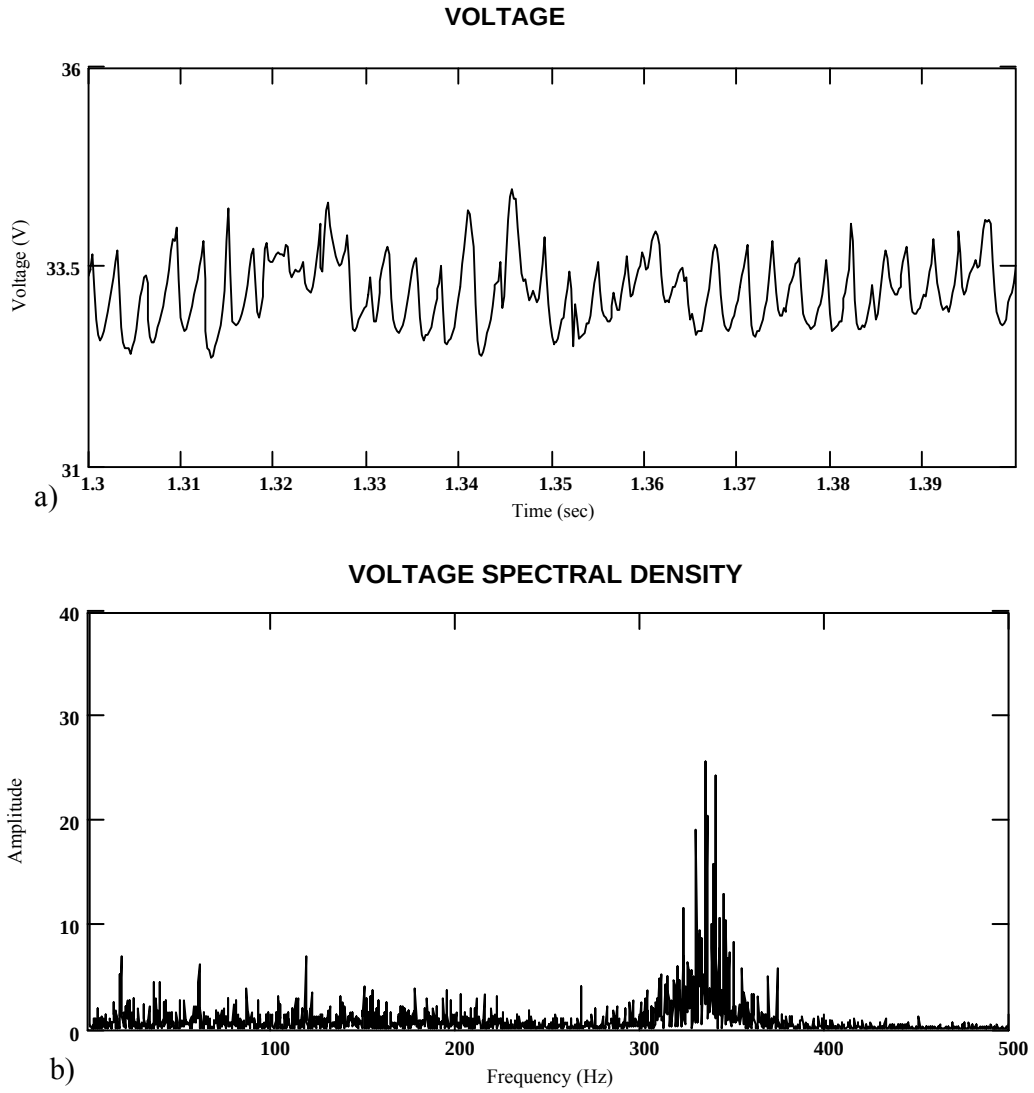

Figure 5.11. a)Voltage signal and b)Fast Fourier Transform of a representative weld made in 90Ar-10CO_2 atmosphere. The voltage signal appears to be fairly periodic, leading to a distinguishing frequency peak in the FFT.

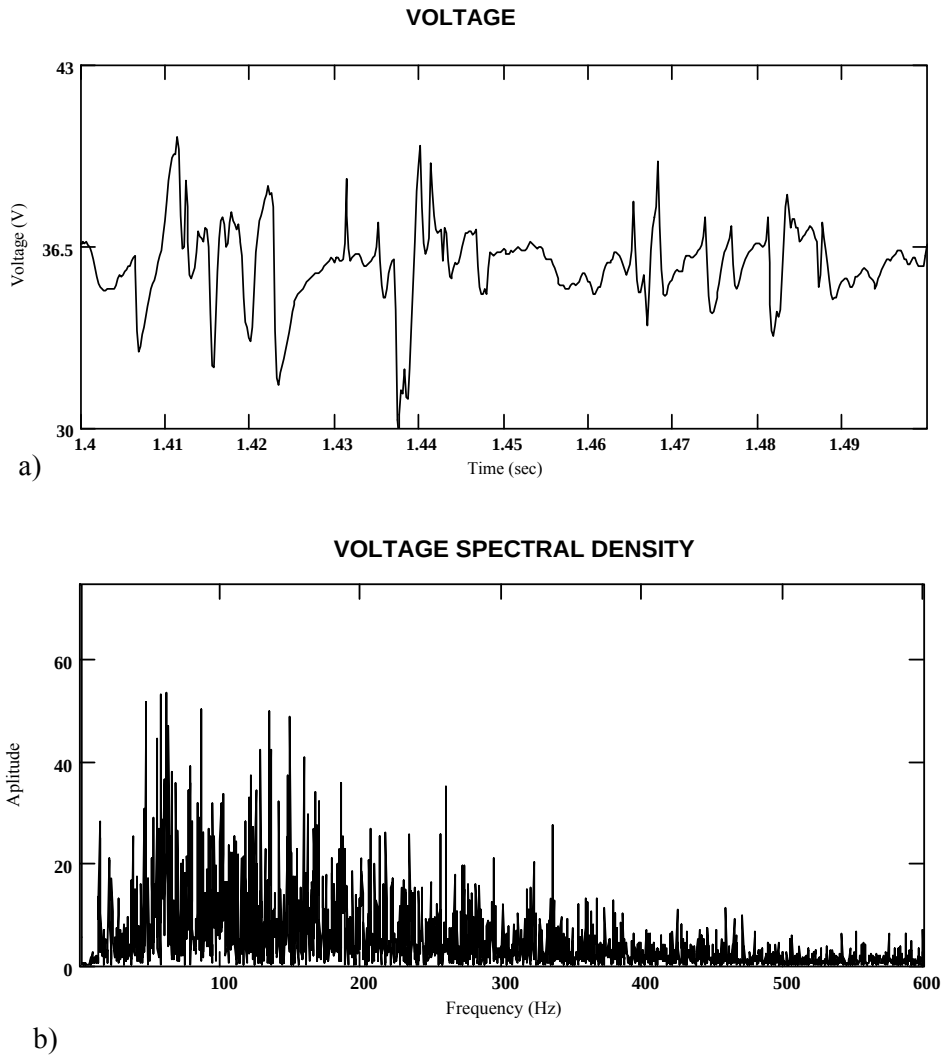

Figure 5.12. a)Voltage and b)FFT of a weld made in 70Ar-30CO_2 atmosphere. The voltage signal is erratic and leads to uncertain frequencies in the FFT.

Once droplet detachment frequency was determined, they were plotted on a graph as a function of current. Figure 5.13 is a representative plot of the transition from low frequency detachments to high frequency detachments. The transition current is determined by taking the average between the upper and lower shelves. In this particular instance the upper shelf begins at 325Amperes. The lower shelf ends at 212 Amperes, so

the transition current is computed as the average of these two numbers, 269 Amperes. Transition currents were determined by this method throughout the research.

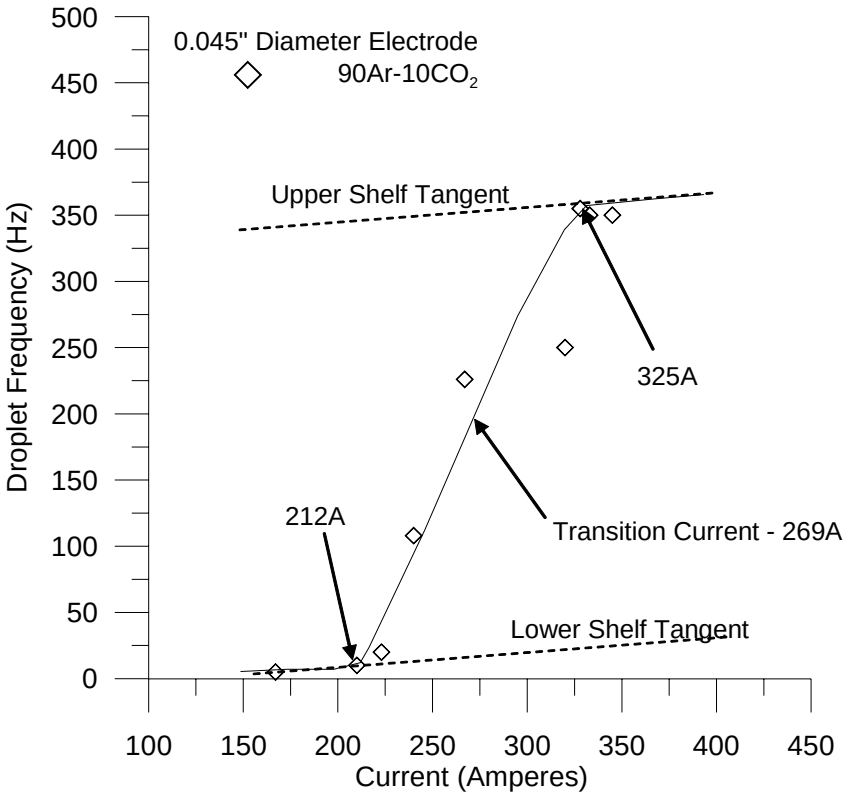

Figure 5.13. A representative plot indicating the variables used in determining the transition current.

Figure 5.14 shows the experimental matrix that was followed throughout the research. Previous published research is shown in the single cross-hatched region. The circles shown on the graph represent particular welding parameters that were used during experimentation. The hollow circles represent parameters that were explored, but not fully investigated. The parameters represented by full circles were fully investigated and the results of these experiments are shown in the next chapter. The double cross-hatched region shows the unexplored parameters, which have not been represented in any

publications to date. This region contains the two smallest wire diameters and various compositions of shielding gas.

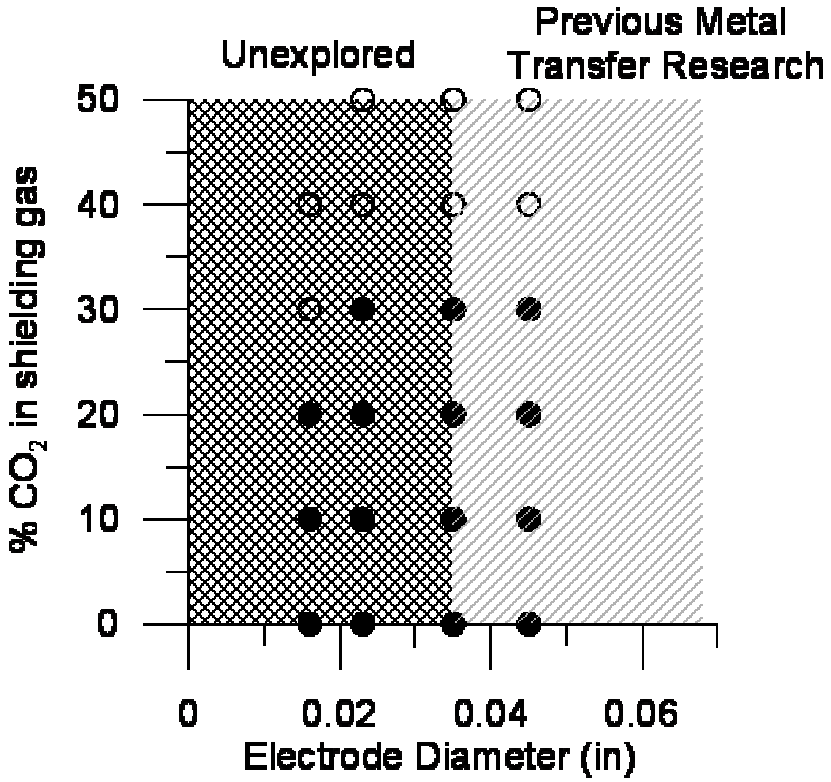

Figure 5.14. The experimental matrix that was used in this research. Solid circles represent full data collection parameters and hollow circles represent exploratory experiments.

6. EXPERIMENTAL RESULTS AND DISCUSSION

Many tests for each setting needed to be performed to get enough data to determine the transition region between globular and spray, even though the only variables that were changed during testing was wire diameter and shielding gas composition. Several trends were exposed and interesting results were found. In the current chapter, the significant patterns in the data and relationships between variables will be summarized. Explanations of these findings are presented, along with comparisons between the predicted and actual behaviors. If differences arise, possible explanations are presented to account for these variances. Following that, limitations that were found during the experimental method are given. Finally, the implications of this research and questions that still remain are discussed.

6.1. Contact Tip Redesign

In this research, the thinnest wire (0.016 in.) was studied using the contact tip described in Section 5.1.3, while the other three thicker wires were studied using a traditional contact tip. It is reasonable to expect this difference to have an effect, especially taking into account that the point of electrical contact for traditional contact tips is 1.25 mm into the tube, as suggested by Waszink and Van den Huevel [41].

This potential difference was tested in this work by performing the same experiments on 0.016 in. diameter wire with both types of contact tips, and all other variables remaining the same. The results are illustrated in Figure 6.1. In this figure, it can be observed that the behavior of both contact tips is essentially the same, but the new

design reaches the same droplet frequencies at currents approximately 10A lower than the traditional contact tip.

The performance of the new contact tip is superior to that of the conventional tube design when using small diameter electrodes. Tests were not performed on larger diameter electrodes, but similar trends may be apparent. The improved performance of this new contact tip suggests that process stability can be improved by precisely controlling the point of current transfer between the contact tip and the electrode as well as reduced downtime due to burnback.

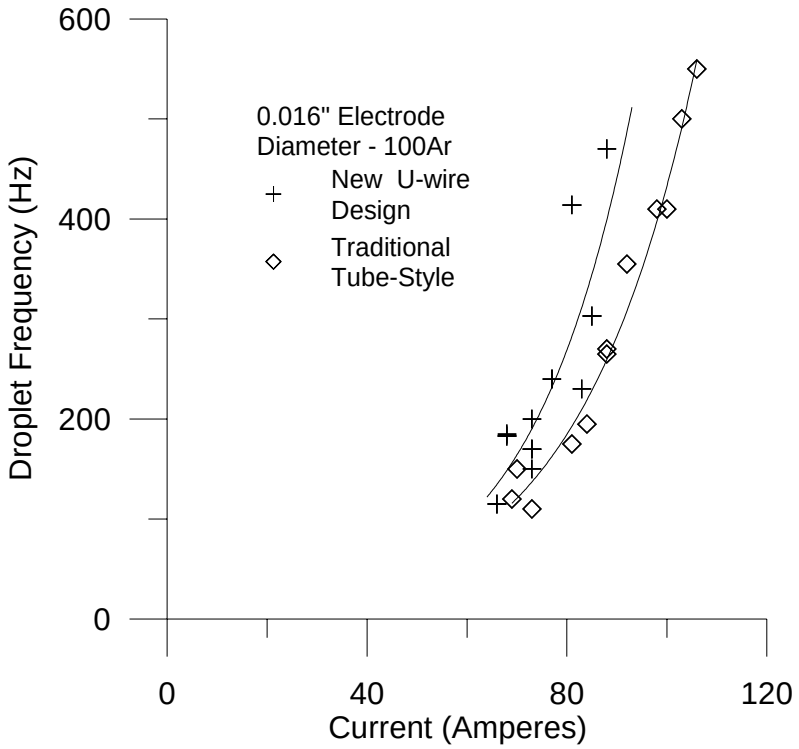

Figure 6.1. A comparison of data collected with two different contact tip designs. The data shows no appreciable difference between the new design and the traditional tube-style.

6.2. Droplet Frequency as a function of Welding Current

Figure 6.2 shows the relationship between droplet frequency and welding current for different diameter electrodes and different shielding gas mixtures. Several distinguishable trends can be noted.

The first pattern is that an increase in CO_2 in the shielding gas results in an increase in transition current. In other words, for a given current, droplet frequency decreases with increasing amounts of CO_2. Along with this observation, the maximum droplet detachment frequency decreased with increasing amounts of CO_2. Both of these trends can be described by an increase in plasma pressure. As higher concentrations of CO_2 are added to the shielding gas, the plasma pressure on the droplet increases, which increases the magnitude of the attaching forces and requires the droplet to grow to a larger size in order to detach. When droplet sizes increase, the droplet detachment frequency decreases. Shielding gas compositions containing more than 30% CO_2 began to exhibit substantial amounts of repelled transfer and are not included in these plots for the 0.045 in., 0.035 in., and the 0.023 in. diameter electrodes. Shielding gas compositions up to 20% CO_2 are shown in Figure 6.2d because 30% CO_2 in the shielding gas produced much spatter and poor weld quality. The droplets produced with the smallest diameter wire produced the smallest droplets, which are more sensitive to plasma pressures. In all cases, increasing the amounts of CO_2 in the shielding gas leads to plasma pressure becoming large enough to suspend the droplet and cause erratic detachment. Other researchers [20, 30] have noted similar findings. The repelled transfer degraded process stability and more spatter was evident in the vicinity of the weld.

As wire diameters decreased from 0.045 in. to 0.023 in., the maximum droplet detachment frequency increased from 350 Hz to over 800 Hz. The maximum droplet detachment frequency for the 0.016 in. diameter electrode was 510 Hz., corresponding to a feedrate of 1443 ipm (0.61 m/s), the maximum limit of the machine. It should also be noted that process stability became difficult to achieve with the smallest diameter wire.

If the process was started with steady-state operation conditions, the electrode would stub the workpiece and the entire length between the contact tip and the workpiece would fragment into liquid droplets. The sequence of events is shown in Figure 6.3. Proceeding from left to right are frame-shots taken from the laser shadowgraph. The time period covered is 0.10 seconds. In order overcome this stubbing and achieve stable operation, the process needed to be started at lower wire feed speeds and welding voltages and then manually adjusted up to the desired testing settings.

This work has shown that a significant shift in metal transfer mode occurs over a relatively short current range in atmospheres containing large amounts of argon (>70%) and the balance CO_2. As current increases, so does the magnitude of electromagnetic pinch force (Lorentz), which is believed to be detaching in argon atmospheres. If this force becomes large enough, it dominates the forces acting on the droplet and causes a large change in droplet mode. These trends extend to 0.016 in. diameter electrodes; however, it is shown in Figure 6.2d that the upper shelf of droplet frequency was not reached. Figure 6.4 shows the transition currents for the three largest electrodes. In this case, the transition current is taken as the average current between the upper and lower shelves of droplet detachment frequency. The smallest electrode is not included because the upper shelf was not found due to limitations in the maximum WFS of the system. Transition currents were not found with shielding gas compositions over 30% CO_2 because repelled transfer became dominant. A dip in transition current can be seen for the 10% CO_2 gas mixture for the 0.023 in. and 0.045 in. wires. Similar to the dip seen in Figure 3.2, this phenomenon can be explained by a reduction in surface tension of the molten steel due to reactions with free oxygen from the dissociation of CO_2 in the plasma. Oxygen is a surface active element that reduces the surface tension of molten steel and allows for easier detachment of the droplet.

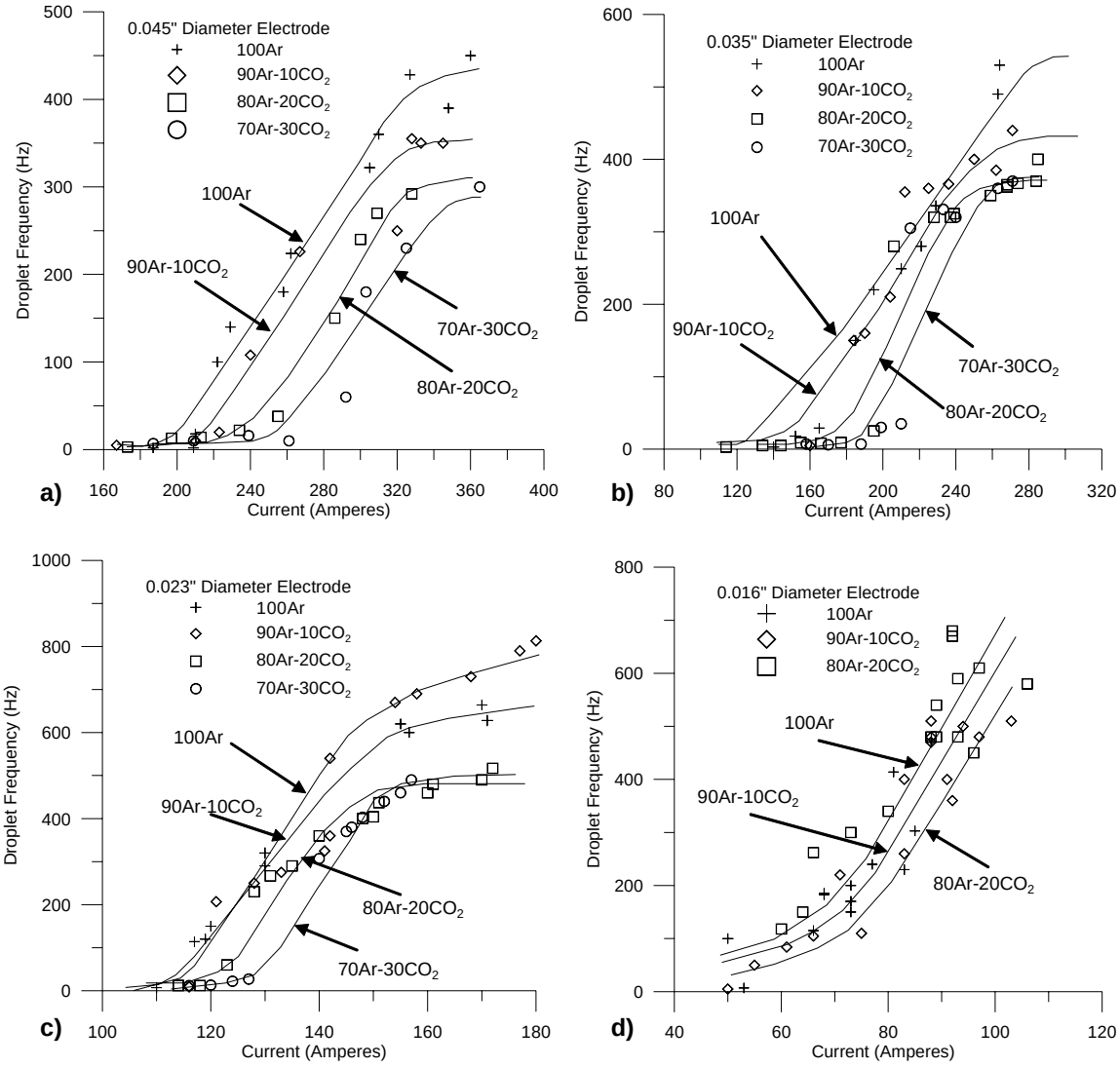

Figure 6.2. The current as a function of droplet frequency graphs for several different wire diameters and shielding gas compositions.

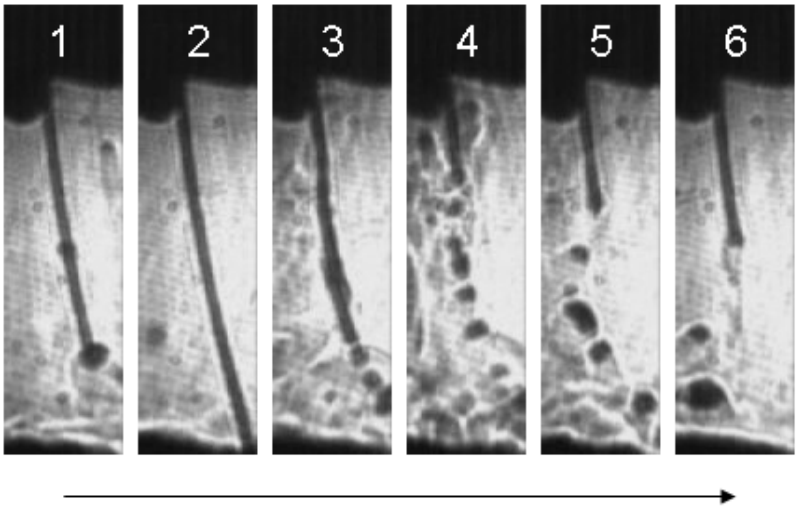

Figure 6.3. Screenshots from the laser shadowgraph that shows the stubbing mechanism. The small wire contacts the baseplate in frame 2 and explodes into small droplets in frame 4. The unstable operating condition continues indefinitely.

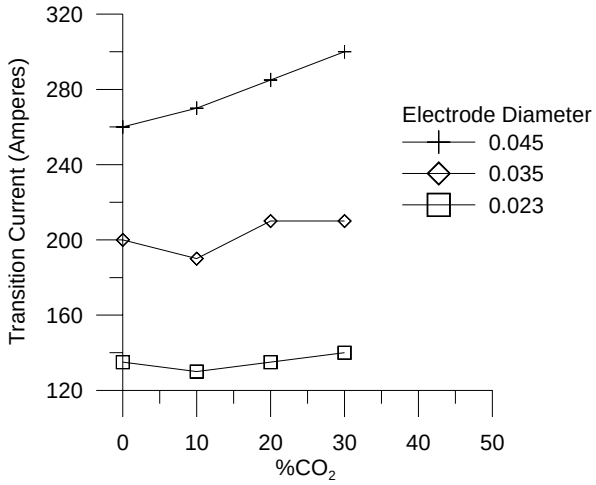

Figure 6.4. Transition currents for various electrode diameters in different composition shielding gases. The transition current here is defined as the average between the upper and lower shelves of detachment frequency. The 0.016 in. wire is not included because the upper shelf was not found.

6.3. Welding Current as a function of Feedrate

Other interesting relationships can be seen with the data that was collected. For instance, by plotting wire feed speed (WFS) as a function of current, a linear trend can be seen. Figure 6.5a shows the current for a given wire feed speed at different gas compositions for the 0.035 in. diameter electrode. Shielding gas composition has little effect on the relationship. This is representative for the other wire diameters as well. Figure 6.5b shows the relationship for different wire diameters. From this relationship, correlations between current and wire feed speed can be made.

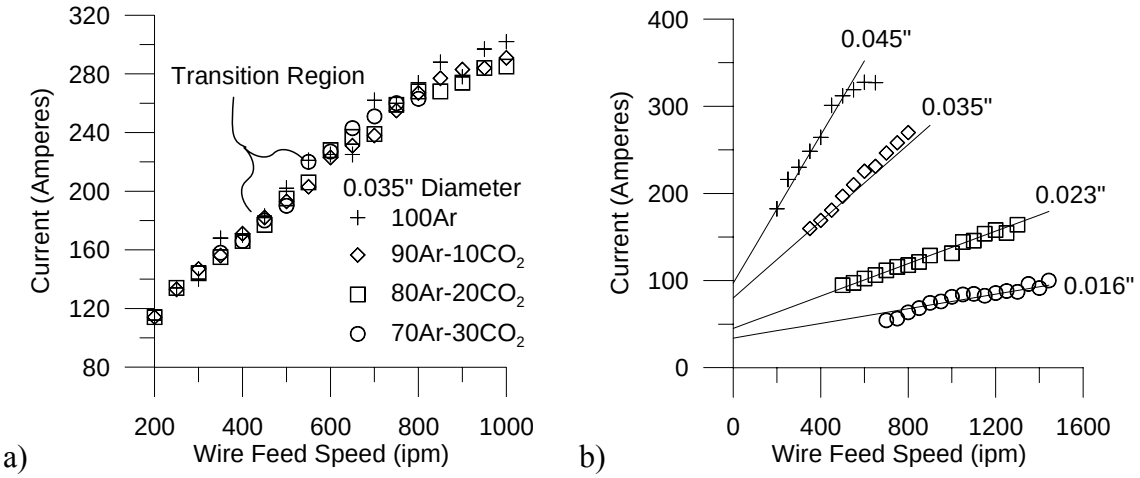

Figure 6.5. (a) Graph showing the relationship between wire feed speed and welding current at various gas composition for 0.035 in. diameter wire. (b) The points are an average of currents for different shielding gas compositions at different wire feed speeds.

6.4. Voltage as a function of Feedrate

Figure 6.6 shows the relationship between voltage and wire feed speed at varying shielding gas compositions and a constant arc length of 0.5 in. The contact tip to work distance was also held constant at 1 in. The particular graph shown uses 0.035 in. diameter wire and is representative of the other wire diameters. Increasing the CO_2

content of the shielding gas requires higher operating voltages to maintain a constant arc length. Wire feed speeds that are less than 400 ipm exhibit a downward trend, but process stability was not good at these low feed rates. The process was not very stable; arc length changed considerably as large droplets detached. As feedrates increased above 400 ipm, the stability increased as well, leading to a very stable arc length. The maximum voltage output of the machine is rated at 40V. For gas compositions containing 20% CO_2 and higher, the output of the machine was maximized for wire feed speed greater than 800 ipm.

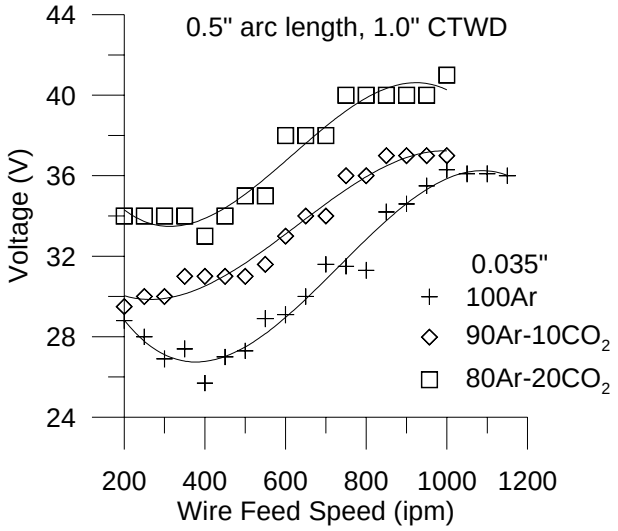

Figure 6.6. The relationship between wire feed speed and voltage for the 0.035 in. diameter electrode at varying gas compositions. The arc length and contact tip to work distance was kept constant

6.5. Droplet Diameter Calculations

To further understand trends in the data and reveal other findings, it is necessary to calculate the average droplet diameter. Direct measurements from the laser-shadowgraph are impractical because of irregularities in the shape as well as visible changes in the droplet diameter due to the Schlieren effect [46]. The droplet diameter, therefore, is calculated from droplet detachment frequency and wire feed speed. By

defining the control volume as the region containing the electrode tip and the detached droplet and neglecting mass losses through evaporation, a volumetric rate balance can be performed, schematically represented in Figure 6.7.

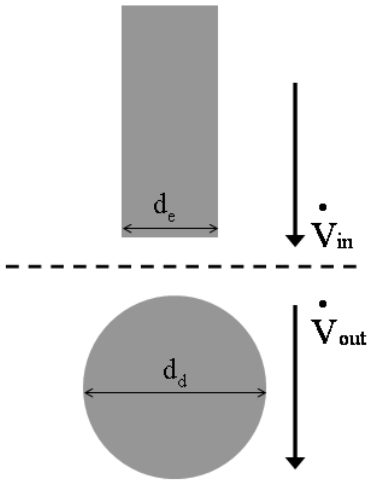

Figure 6.7. The schematic representation of the volumetric rate balance used to calculate the droplet diameters.

The equation is given as:

$$d_d = \left(\frac{WFS \cdot d_e^2}{40 \cdot f_d} \right)^{1/3} \qquad 6.1$$

where d_d is the droplet diameter, WFS is wire feed speed (in/min), d_e is electrode diameter and f_d is the droplet detachment frequency. For typical droplet sizes, the error in droplet detachment frequency (±5%) translates to an error in droplet diameter of ±0.001 inch.

6.6. Droplet Diameter as a function of Welding Current

Equation 6.1 shows an inverse relationship between droplet diameter and droplet detachment frequency. Figure 6.8 shows this relationship graphically. This graph shows the droplet diameters at various welding currents for the 0.023 in. diameter electrode in a variety of shielding gas compositions. At 70Ar-30CO_2, repelled transfer began to occur.

Higher concentrations of CO_2 resulted in excessive amounts of spatter and erratic droplet detachment. At low welding currents, the droplet detachment frequency is low and droplet diameters are high. As welding current increases, droplet diameters decrease substantially and droplet frequency increases. At the higher operating currents, the droplet diameters begin to become less dependent on the welding currents. In this graph, it also appears that shielding gas composition has little effect on the transition from globular to spray. When calculating the droplet diameters, a change of 100 Hz in droplet detachment frequency in the transition region results in a change in droplet diameter of 0.002 in. Figure 6.1c shows that the range of frequencies is about 200 Hz between the 100Ar and 70Ar-30CO_2 in the transition region. This correspond to a change in droplet diameter of about 0.004 in. This small change is not apparent in Figure 6.7, which is why it appears that shielding gas composition has little effect on the transition.

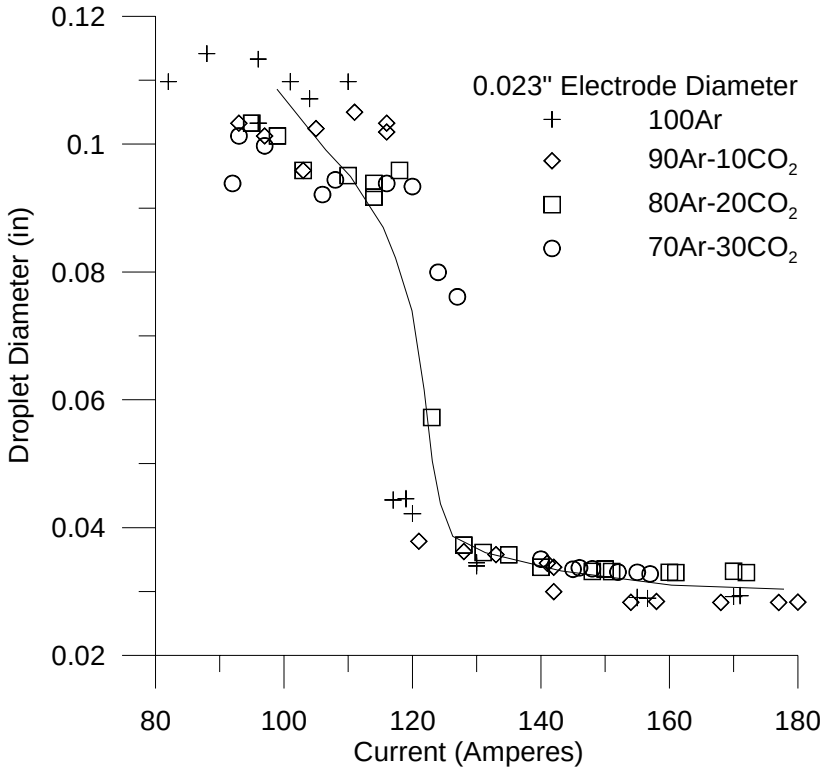

Figure 6.8. Droplet diameter at varying welding currents and gas compositions. The droplet diameter is influenced greatly by welding current. Shielding gas composition appears to have limited effects.

Figure 6.9 shows the current/droplet diameter characteristics for all four wire diameters in a 90Ar-10CO_2 gas atmosphere. They all exhibit the same trends discussed above. Increasing welding current decreases droplet diameter until the diameters level off at high operating currents. As electrode diameter decreases, so does the droplet sizes at high currents.

It is interesting to note that the droplet diameters do not become smaller than wire diameters with the three smallest electrodes. This work shows for the first time that for relatively thin electrodes (typically less than 0.045 in. diameter) a transfer mode that involves both tapering and droplets larger than the wire.

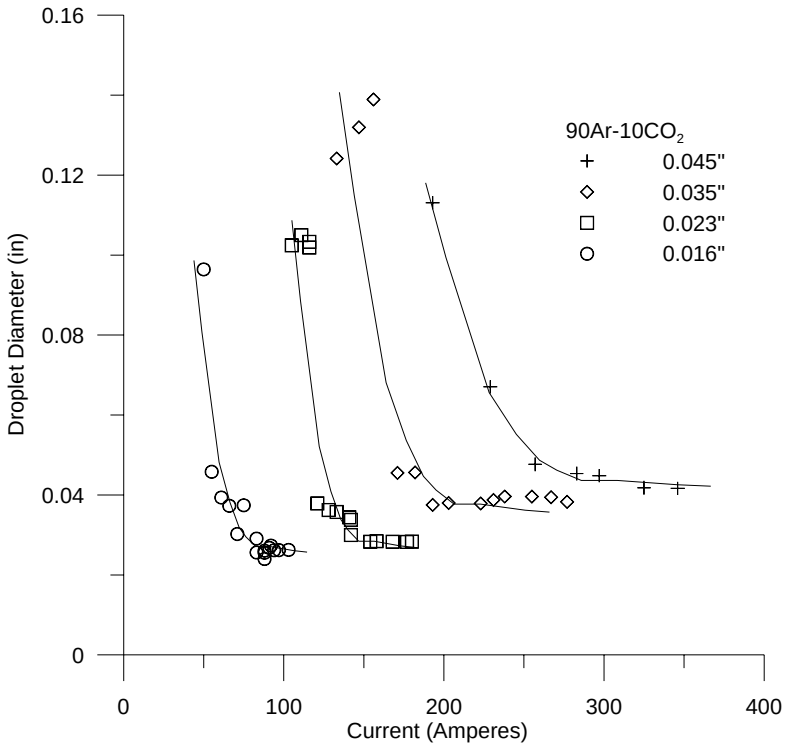

Figure 6.9. Compilation of data for all wire diameters. As welding current increases, the transfer mode shifts from large diameter droplets to small diameter droplets for all wire diameters.

6.7. Droplet Diameter as a function of Feedrate

The relationship between droplet diameter and feedrate is similar to that between droplet diameter and current. Figure 6.10 shows four separate graphs, representing the four different wire diameters that were used in the study. In Figure 6.9a, the droplet diameters become smaller than the electrode diameter (0.045 in.) at a feedrate of 400ipm. The rest of the electrode sizes do not exhibit this same behavior. They do show a decrease in the droplet diameter sizes, but never to the point at which the droplets become smaller than the electrode. Figure 6.11 is a combination of all the diameters on one graph. The tendency is that the droplets, regardless of wire diameter, seem to be limited to a similar size at high wire feed speeds.

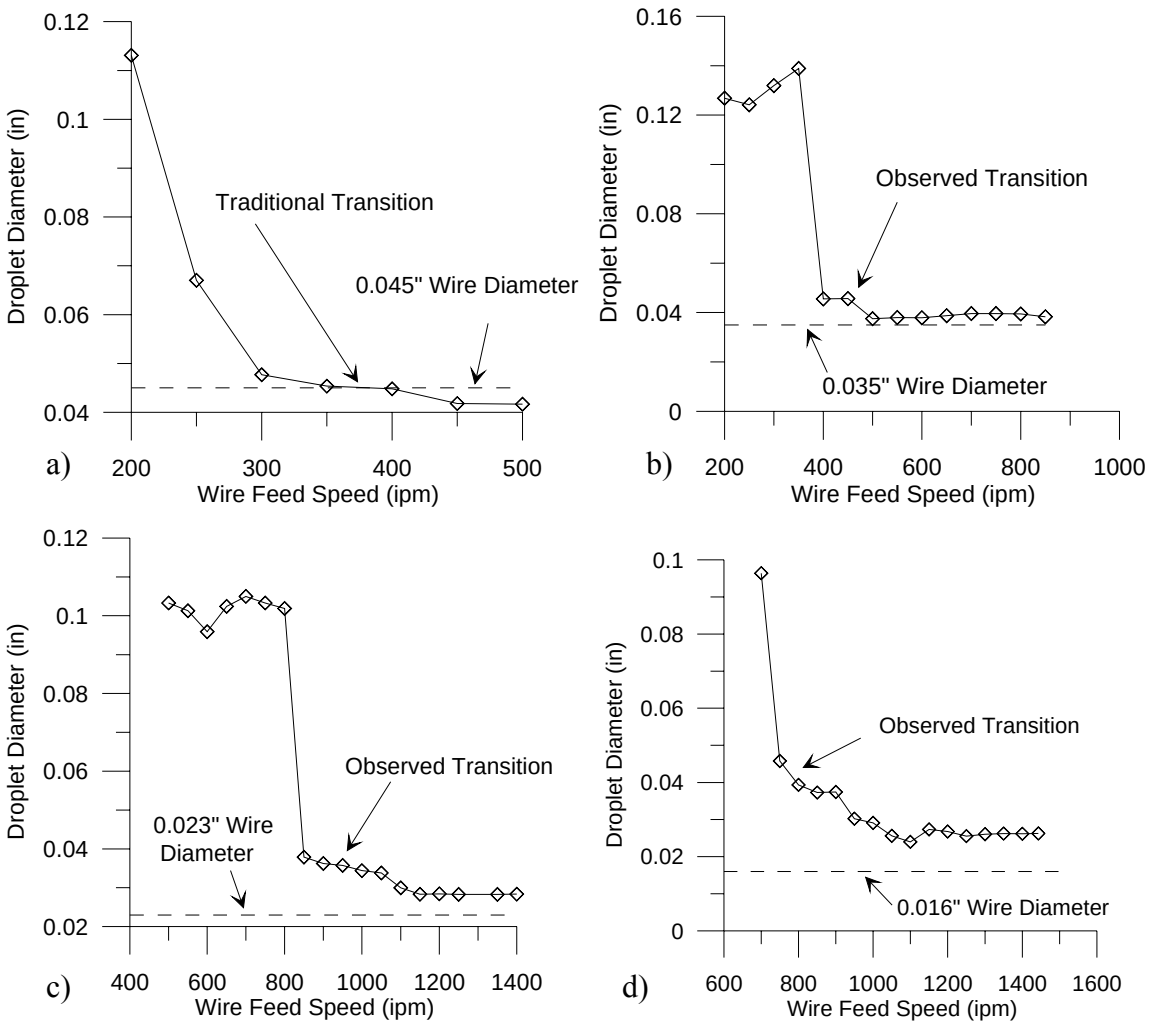

Figure 6.10. Characteristics between droplet diameter and wire feed speed for four different electrode diameters. Shielding gas compositions are 90Ar-10CO_2. Droplet diameters never become smaller than wire diameters in the three smallest electrodes.

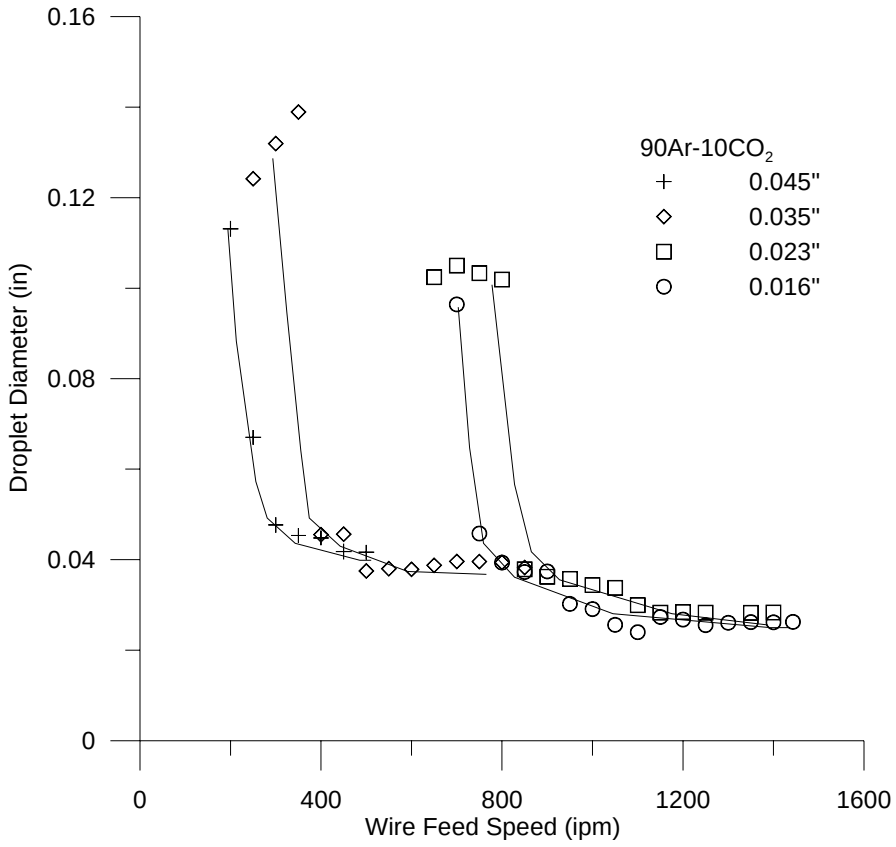

Figure 6.11. Droplet diameter sizes at different feedrates for four different wire diameters.

6.8. Effects of Carbon Dioxide

At CO_2 concentrations of 30% or higher, repelled transfer becomes detrimental to the welding process. As the compositions increase, one distinguishing change occurs: The properties of the plasma which has several consequences. As the constituents of the shielding gas vary, so do the properties of the plasma within it, notably the thermal and electrical conductivity. Carbon dioxide also dissociates at elevated temperatures. It is possible that plasma pressure increases to a point that it is able to suspend the droplet. This observation is consistent with what is seen easily in the laser shadowgraphs. The mechanism for this pressure increase is still debated.

6.9. Comparison between Predicted and Actual Results

The hypothesis stated:

> To offset the constricted arc typical of high CO_2 concentrations, thinner wire diameters will be used. It is expected that the arc will be forced to climb the electrode to maintain a constant current density. As the arc climbs over the droplet, transition will occur and spray transfer will be the dominant metal transfer mode.

This was schematically shown in Figure 4.3. Our research found that this hypothesis is attainable only partially, because below a given wire diameter, the molten droplet diameter at the electrode tip does not decrease in size in proportion to decreases in wire diameter. Figure 6.13 shows the results in a schematic diagram. By using wire diameters as thin as 0.016 in., spray transfer was not achieved in high CO_2 concentrations. It was assumed that smaller electrode diameters would produce smaller droplet diameters, but this assumption was shown to be not the case. Minimum droplet diameters did not decrease proportionally to the decrease in wire diameter. While operating, the process sounded and appeared to be spray transfer mode, however, through analysis the visible boundaries of the arc do not coincide with a particular transfer mode, as previously thought.

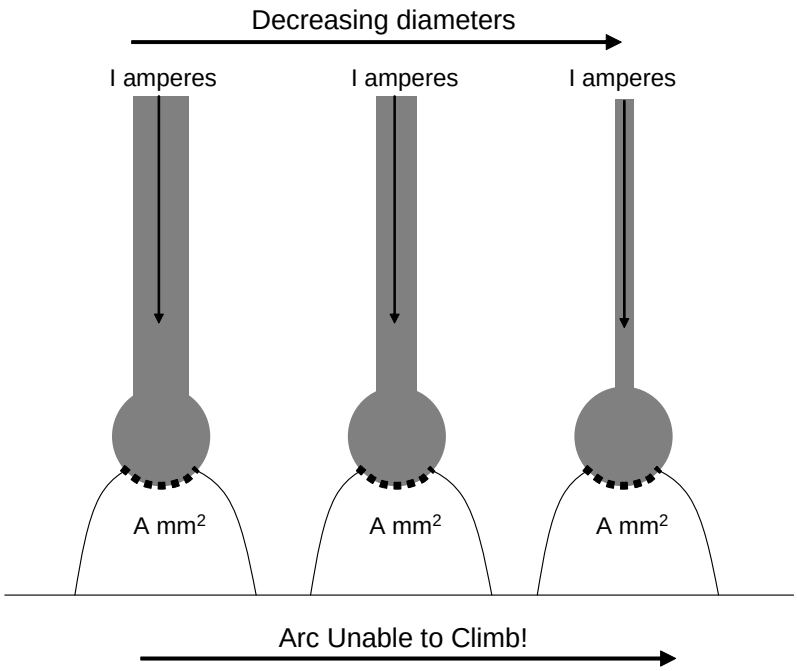

Figure 6.12. The arc is unable to climb up and envelope the droplet because droplet sizes do not decrease as wire diameter decreases. Figure is not to scale.

6.10. Limitations in Methods or Materials

During the experiments, the limitations of the welding machines were exceeded multiple times. Through many modifications, these machines evolved so that they could perform the tasks needed. Even so, the 0.016 in. diameter electrode was pushing the limits of the experimental setup. The availability of the thin wire was also an issue, taking almost two months to find a supplier.

The data collected showed noticeable trends, but further statistical analysis can be done to improve the ranges. Data presented here did was not subjected to any statistical analysis tools. The scatter that shows up comes from variability in the welding process itself. From day to day, variables change. Atmospheric conditions, variability in materials such as shielding gas, surface condition can all have slight changes in the

welding process. By improving these methods and materials, the data could be held to higher tolerances.

6.11. Summary

The new designed contact tip gave similar results to traditional tube designs, but with greater process stability with thin electrodes. As wire diameters decrease, so does the transition current from low frequency detachments to high frequency detachments. The droplet diameters for the 0.035 in. and smaller electrodes never became smaller than the electrode diameters, even at very high feedrates. Shielding gas compositions containing more than 30% CO_2 exhibited repelled transfer, regardless of electrode diameter. CO_2 does not significantly affect the transition current.

7. CONCLUSIONS AND RECOMMENDATIONS

7.1. Conclusions

In conclusion, this investigation has revealed several interesting characteristics through the study of GMA welding using small diameter electrodes. They include the following:

- The droplet diameter does not become smaller than the electrode diameter for electrodes of 0.035 in. and smaller for welds made in the flat position and non-pulsed power. A lower limit exists for droplet sizes that follows a similar trend, regardless of electrode diameter. The primary focus in this investigation is the transition from globular to spray as current is increased. Swirling or rotating spray was not considered due to the fact that droplets cease to form and instead are replaced by long liquid tails.
- New observations have been made in metal transfer modes. By using small diameter electrodes (<0.035 in.) with shielding gases containing more than 70% argon, the mode has characteristics of both globular and spray. To an experienced welding operator, the transfer mode looks and sounds like spray. This is due to the fact that the operation is very stable and the arc attaches above the droplets. Also, the droplet detachment frequency is in excess of 400 Hz, making it sound like spray transfer. However, through further analysis with high speed video and voltage processing, it is found that the droplet diameters are not smaller than the wire diameters. This last finding would traditionally define the mode as globular.

- A special contact tip was designed for use with the 0.016 in. diameter electrode because no commercially produced tips were available. When compared to the conventional tube-style, the new design produced similar results and better performance. Burnback was less frequent and downtime was kept to a minimum. This new design currently has a patent pending.
- Thinner diameter electrodes lower the transition current from small droplet detachment frequencies to high droplet detachment frequencies. A 0.045 in. diameter electrode operating in 90Ar-10CO_2 shielding gas has a transition current of 280 Amperes. In comparison, the 0.023 in. diameter electrode transitioned at 130 Amperes.

7.2. Recommendations

Further modifications to the machine setup can be made. Incorporating an even faster wire feeder can expand the data range even further. Along with this, the power supply would need to be upgraded to ramp-up the current and prevent stubbing.

Coatings on the wire, as done by Lesnewich [1], may influence the metal transfer substantially. Changing the plasma properties directly around the anode tip can influence the flow of current and the effective droplet detachment forces.

An improved method of determining the droplet detachment frequency is another suggestion for future work. Two methods were compared and found to be only 10% different, yet the data collected was still scattered. Is it variability in the process or the analysis?

Previous experimental observations need to be qualified for the particular size welding electrode. Small diameter electrodes have similarities and differences to their larger counterparts. Through this investigation, the feasibility of the process has been shown to work. Further investigation is needed to qualify the process and its applications.

REFERENCES

1. Lesnewich, A., *Electrode Activation for Inert-Gas-Shielded Metal-Arc Welding.* Welding Journal, 1955. **35**(12): p. 1167-1178.
2. Cushman, E., *Electrode for Spatter-Free Welding of Steel in Carbon Dioxide.* Welding Journal, 1961. **41**(1): p. 14s-21s.
3. Rothschild, G.R., *Carbon-Dioxide-Shielded Consumable-Electrode Arc Welding.* Welding Journal, 1956. **35**(1): p. 19-29.
4. Fanyo, L. and E. Plute, *An Investigation of the U.S. Welding Market: Possible Applications for a Modified Welding Machine for High Quality Welds Using Inexpensive Gas*. 2004, Colorado School of Mines: Golden, CO.
5. Adam, G., Siewert, T.A., *Sensing of GMAW Droplet Transfer Modes Using an ER100S-1 Electrode.* Welding Journal, 1990. **69**(3): p. 103s-108s.
6. Allemand, C.D., R. Schoeder, D.E. Ries, and T.W. Eagar, *A Method of Filming Metal Transfer in Welding Arcs.* Welding Journal, 1985. **64**(1): p. 45-47.
7. Smartt, H.B., C.J. Einerson, A.D. Watkins, and R.A. Morris. *Gas Metal Arc Process Sensing and Control*. in *International Conference on Trends in Welding Research*. 1986. Gatlinburg, TN: ASM International.
8. Baune, E., C. Bonnet, and S. Liu, *Assessing metel transfer stability and spatter severity in flux cored arc welding.* Science and Technology of Welding and Joining, 2001. **6**(3): p. 139-148.
9. Ushio, M., K. Ikeuchi, M. Tanaka, and T. Seto, *Effects of Shielding Gas on Metal Transfer.* Welding International, 1995. **9**: p. 462-466.
10. Madigan, B.R. 1994. *Control of Gas Metal Arc Welding Using Arc Light Sensing*. Phd. Thesis, Colorado School of Mines, Golden, CO.
11. Lancaster, J.F., *The Physics of Welding*. 2nd ed. 1986: Pergamon Press. 341.
12. Brandi, S., C. Taniguchi, and S. Liu, *Analysis of Metal Transfer in Shielded Metal Arc Welding.* Welding Journal, 1991. **70**(10): p. 261s-270s.
13. Liu, S. and T.A. Siewert, *Metal Transfer In Gas Metal Arc-Welding - Droplet Rate.* Welding Journal, 1989. **68**(2): p. S52-S58.
14. Spraragen, W., Bela A. Lengyel, *Physics of the Arc and the Transfer of Metal in Arc Welding.* Welding Journal 1943. **22**(1): p. 2-42.
15. Muller, A., W.J. Greene, and G.R. Rothschild, *Characteristics of Inert-Gas-Shielded Metal Arcs.* Welding Journal, 1951. **31**(8): p. 717-727.
16. Ludwig, H.C., *Current Density and Anode Spot Size in the Gas Tungsten Arc.* Welding Journal, 1968. **48**(5): p. 234s-240s.

17. Waszink, J.H. and M.J. Piena, *Experimental Investigation of Drop Detachment and Drop Velocity in GMAW*. Welding Journal, 1986. **65**(11): p. 289s-298s.
18. Kim, Y.S. and T.W. Eagar, *Analysis of Metal Transfer in Gas Metal Arc-Welding.* Welding Journal, 1993. **72**(6): p. S269-S275.
19. Amson, J.C., *Lorentz force in the molten tip of an arc electrode.* British Journal of Applied Physics, 1965. **16**: p. 1169-1179.
20. Nemchinsky, V.A., *The effect of the type of plasma gas on current constriction at the molten tip of an arc electrode.* Journal of Physics D: Applied Physics, 1996. **29**: p. 1202-1208.
21. Lan, H.-G. 1988. *Metal Transfer in Gas Metal Arc Welding*. M.S. Thesis, Colorado School of Mines, Golden, CO.
22. Heald, P.R., R.B. Madigan, T.A. Siewert, and S. Liu, *Droplet Transfer Modes for a Mil 100S-1 GMAW Electrode*. 1991, NIST: Boulder, CO.
23. Lesnewich, A., *Control of Melting Rate and Metal Transfer in Gas-Shielded Metal-Arc Welding Part I - Control of Electrode Melting Rate.* Welding Journal, 1958. **37**(8): p. 343s-353s.
24. ASM International, *Welding, Brazing, and Soldering*. 1st ed. ASM Handbook. Vol. 6. 1993: ASM International.
25. Lesnewich, A., *Control of Melting Rate and Metal Transfer in Gas-Shielded Metal-Arc Welding Part II - Control of Metal Transfer.* Welding Journal, 1958. **37**(9): p. 418s-425s.
26. *Welding Handbook*. Fundamentals of Welding, ed. C. Weisman. Vol. 1. 1981, Miami, FL: AWS.
27. Rhee, S. and E. Kannatey-Asibu, *Observation of Metal Transfer during Gas Metal Arc Welding.* Welding Journal, 1992. **71**(11): p. 381-386.
28. Waszink, J.H. and L.H.J. Graat, *Experimental Investigation of the Forces Acting on a Drop of Weld Metal.* Welding Journal, 1983. **62**(4): p. 108s-116s.
29. Rhee, S. and E. Kannateyasibu, *Analysis Of Arc Pressure Effect On Metal Transfer In Gas-Metal Arc-Welding.* Journal Of Applied Physics, 1991. **70**(9): p. 5068-5075.
30. Mechev, V.S., A.A. Valeeva, A.Z. Zhainakov, V.S. Slobodyanyuk, M.A. Samsonov, and V.S. Engelsht, *The Thermal And Physical-Properties Of Gaseous Carbon-Dioxide And Their Effects On The Welding Arc.* Automatic Welding USSR, 1982. **35**(4): p. 24-29.
31. Haidar, J. and J.J. Lowke, *Effect of CO2 Shielding Gas on Metal Droplet Formation in Arc Welding.* IEEE Transactions on Plasma Science, 1997. **25**(5): p. 931-936.
32. Ludwig, H.C., *Plasma-Energy Transfer in Gas-Shielded Welding Arcs.* Welding Journal, 1959. **39**(6): p. 296s-300s.
33. Cary, H.B., *Modern Welding Technology*. Fourth ed. 1998, NJ: Prentice Hall. 780.

34. Cuiuri, D., J. Norrish, C. Cook, *New approaches to controlling unstable Gas Metal Arc Welding.* Australasian Welding Journal, 2002. **47**(3): p. 39-47.
35. Smith, A.A., *CO_2 welding of steel*. 3 ed. 1971, Cambridge, UK: The Welding Institute.
36. Mendez, P.F., M.A. Ramirez, G. Trapaga, and T.W. Eagar, *Order of Magnitude Scaling of the Cathode Region in an Axisymmetric Transferred Electric Arc.* Metallurgical Transactions B, 2001. **32B**: p. 547-554.
37. Needham, J.C. and A.W. Carter, *Arc and transfer characteristics of the steel/CO_2 welding process.* British Welding Journal, 1967(October): p. 533-549.
38. Matsuda, F., M. Ushio, H. Nishikawa, T. Yokoo, *Pulsed GMAW - Spattering in Pulsed CO_2 Welding.* Transactions of JWRI, 1985. **14**(1): p. 13-19.
39. Miller Electric Mfg. Co., *Miller Maxtron 450 Owner's Manual - OM-2206B*. 1993.
40. Miller Electric Mfg. Co., *Miller S-70 Owner's Manual - OM-223 605A*. 2006.
41. Waszink, J.H. and G.J.P.M. Van den Heuvel, *Heat Generation and Heat Flow in the Filler Metal in GMA Welding.* Welding Journal, 1982: p. 269s-282s.
42. Mendez, P.F. and E. Soderstrom, *Gas metal arc welding methods and apparatus*, United States Patent Application # 2006/0237411 A1.
43. Johnson, J.A., N.M. Carlson, H.B. Smartt, and D.E. Clark, *Process Control of GMAW: Sensing of Metal Transfer Mode.* Welding Journal, 1991. **70**(4): p. 91s-99s.
44. Wang, W., S. Liu, and J.E. Jones, *Flux-Cored Arc-Welding - Arc Signals, Processing And Metal Transfer Characterization.* Welding Journal, 1995. **74**(11): p. 369s-377s.
45. Kohn, G. and T.A. Siewert. *The Effect of Power supply Response Characteristics on Droplet Transfer of GMA Welds*. in *International Conference on Trends in Welding Research*. 1986. Gatlinburg, TN: ASM International.
46. Settles, G.S., *Schlieren and Shadowgraph Techniques : Visualizing Phenomena in Transparent Media*. 2001: Springer.